Manuscript Details

Manuscript number	EUROPOL_2019_535_R1
Title	Eugenol-based thermally stable thermosets by Alder-Ene reaction: from synthesis to thermal degradation
Article type	Research paper

Abstract

Performing thermostable materials such as phenolic or epoxy networks are classically obtained from petrobased and harmful monomers. In this study, alternative solutions based on renewable eugenol trifunctional monomer (TEP) are proposed. Thus, innovative biobased Alder-ene thermosets are prepared by reacting TEP with two different bismaleimides : N,N'-1,3-phenylene bismaleimide (PhBMI) and polydimethylsiloxane bismaleimide (SiBMI) leading to different crosslinked aromatic networks. These materials exhibit various mechanical properties with very different Tg values of -113°C and 247°C for SiBMI and PhBMI materials respectively. However, both thermosets exhibit excellent thermal properties with elevated degradation temperature and high char yield. The degradation behavior was studied using thermogravimetric analysis – Fourier transformed infrared spectroscopy (TGA-FTIR): only silicon compounds were observed for SiBMI, whereas phosphorus and carbonaceous products had specific signatures in degradation gases for PhBMI. Kinetic analysis of degradation confirmed those different behaviors. Our contribution with two original Alder-ene thermosets is an innovative way to develop sustainable versatile high-performant materials.

Keywords	Biobased; Alder-ene; eugenol; thermal properties; maleimide; thermoset
Manuscript category	Regular Paper
Corresponding Author	Sylvain CAILLOL
Corresponding Author's Institution	ICGM
Order of Authors	Mélanie Decostanzi, Romain Tavernier, Gaelle Fontaine, Serge Bourbigot, Claire Negrell, Sylvain CAILLOL
Suggested reviewers	Jean-Marie Raquez, Luc Averous, Giuseppe Palmese, fouad laoutid, Abdelghani Laachachi, Joseph Stanzione

Submission Files Included in this PDF

File Name [File Type]

cover letter.doc [Cover Letter]

Answer to reviewer.doc [Response to Reviewers]

Highlights.docx [Highlights]

Eugenol AlderEne revised.docx [Manuscript File]

Eugenol AlderEne revised yellow.docx [e-Component]

Submission Files Not Included in this PDF

File Name [File Type]

GA.png [Graphical Abstract]

To view all the submission files, including those not included in the PDF, click on the manuscript title on your EVISE Homepage, then click 'Download zip file'.

Dr Sylvain CAILLOL
Sylvain.caillol@enscm.fr
Tel: (+33) 4-6714-4327
Institut Charles Gerhardt Montpellier
UMR 5253 CNRS-UM-ENSCM
8 rue de l'Ecole Normale
34296 Montpellier - France

Montpellier, March, 19th 2019

To Prof Mike Shaver
Editor of European Polymer Journal

Dear Prof Mike Shaver,

May I draw your attention on a manuscript entitled "Eugenol-based thermally stable thermosets by Alder-Ene reaction: from synthesis to thermal degradation" that my co-workers and I would like to submit to European Polymer Journal?

Alder-ene reactions were initially used in order to improve properties of phenolics. For example allylation of the phenol moiety, and subsequent cure reaction with bismaleimide, or functionalization of the phenolic polymers by both allyl and maleimide moiety result in Phenol-Maleimidophenol-Allylphenol-Formaldehyde thermosets.

The use of biobased chemicals has become an important area in polymer research, in order to lower the environmental impacts of resulting materials. Moreover, investigation on new biobased molecules for polymers with new properties is also gaining increasing interest, especially in thermosets field. Several studies have been conducted on the synthesis and polymerization of aromatic biobased monomers, in order to obtain thermosetting materials with enhanced properties, for example using vanillin, or other lignin derivatives, cardanol, or tannins. Eugenol, an allyl natural phenol easily extracted from cloves, is of prime interest for bismaleimide (BMI) chemistry, indeed it is used for the synthesis of BMI thermosets. Eugenol-based monomers can be cured with bismaleimides, resulting thermally stable materials with high char yields.

In the present study, we used trieugenol phosphate monomers, which we recently reported for expoy networks, with two different bismaleimides in order to synthesize novel Alder-ene thermosets. We studied the influence of the bismaleimide structure on the performances and degradation behavior of the materials. In one hand, we used a commercially available aromatic bismaleimide, the N,N'-1,3-phenylene bismaleimide (PhBMI), in order to obtain high Tg material, and on the other hand, we synthesized a new polydimethylsiloxane-containing bismaleimide (SiBMI), resulting in a very low Tg material. We analyzed the thermo-mechanical properties and studied the degradation of those thermosets.

I trust that this manuscript is of interest for the scientific community (both academia and industry) since this manuscript displays a balance between theoretical aspects of the synthesis of aromatic monomers and their interest for the synthesis of aromatic polymers. Additionally, this article will attract various academic teams and industries especially producers of monomers or polymers such as Dupont (USA), Huntsman (Europe and USA), Dow Chemical (USA), Valspar (USA), and BASF (Germany) and Mitsui (Japan) but also end-users such as automotive, building/packaging and electronics industries.

I thank you very much for your kind attention in considering my paper.

Yours Sincerely,

Dr HDR Sylvain CAILLOL

Dr Sylvain CAILLOL
Sylvain.caillol@enscm.fr
Tel: (+33) 4-6714-4327
Institut Charles Gerhardt Montpellier
UMR 5253 CNRS-UM-ENSCM
8 rue de l'Ecole Normale
34296 Montpellier - France

Montpellier, May, 9th 2019

To Prof Mike Shaver
Editor of European Polymer Journal

Dear Prof Mike Shaver,

First of all, I want to thank the reviewers for the quality of the reviewing process as interesting comments have been made and helped to improve our paper. We have thus replied to each reviewer by taking each point one by one and by making the required changes in yellow in the revised version of our manuscript.

Reviewer 1
- This paper revisits the classical Alder-Ene reaction.
Some typos must be corrected.
➤ We checked grammar and spelling and corrected manuscript accordingly.

The authors must use IUPAC recommendations: Molecular weight must be replaced by Molar mass, and so on ...
➤ We checked manuscript according to IUPAC recommendations and corrected the article accordingly.

Figure 11 is not clear for the reader (too small ...)
➤ In order to clarify figures, we separated Figure 10-a and 10-b that are now Figure 10 and Figure 11. We also separated former Figure 11-a and Figure 11-b that are now Figure 12 and Figure 13. We improved former Figure 10-a and 11-a (TGA of both thermosets under N_2 with several heating rates), but we are not able to redraw former figures 10-b and 11-b (DTG and fits) because of a software issue that does not allow us to generate raw data. We may be able to correct those figures later (for proofreading).

Reviewer 2
- Overall, the manuscript fits within the scope of the European Polymer Journal. It is well written and easy to follow with only minor edits needed to improve grammar and formatting. It demonstrates the ability to incorporate bio-based components into high performance (high thermally stable) thermosetting polymers. However, in order to enhance and broaden the scientific impact of the research presented, the following recommendations are encouraged to consider:

1.   Review manuscript to improve grammar and formatting (all according to the Guidelines for Authors)
   ➢ We checked grammar and spelling and corrected manuscript accordingly.

2.   More details are needed with regards to error and error analyses, especially for the DSC and DMA data
   ➢ We corrected the measured values accordingly with one standard deviation uncertainty. For Tg determination by DSC, we performed 3 integrations and used the mean value, with standard deviation. For E' values measured by DMA, we determined the values on the plateau at 3 different temperatures all along the plateau. Displayed values are now mean values, with standard deviation.

3.   Graphs need to be improve for ease of reading the understanding. Most seem to be created via Excel and are of relatively poor quality. Consider using another graphing program such as Origin or MATLAB, all the while following the Guidelines for Authors.
   ➢ In order to clarify figures, we separated Figure 10-a and 10-b that are now Figure 10 and Figure 11. We also separated former Figure 11-a and Figure 11-b that are now Figure 12 and Figure 13. We improved former Figure 10-a and 11-a (TGA of both thermosets under N2 with several heating rates), but we are not able to redraw former figures 10-b and 11-b (DTG and fits) because of a software issue that does not allow us to generate raw data. We may be able to correct those figures later (for proofreading).

4.   More information is needed about the DMA experiments. Also, were the DMA experiments conducted via the guidelines suggested by McAninch et al? (https://onlinelibrary.wiley.com/doi/10.1002/pen.24167)
   ➢ We understand the issue raised by Reviewer 2. In fact, we were not able to perform DMA analysis using single cantilever because our laboratory does not have the equipment. However, measurements using Metravib DMA Machine fully respects the standard ISO 6721.4, and the samples we used respected a shape factor according to the specification of the machine. We thus included more details about the samples and the shape factor requirements met by our samples.

5.   The Results and Discussion section seems to be a little unorganized/choppy. Consider reorganizing from monomer/oligomer, to cure/cure kinetics, to swelling/gel, to TGA, to DMA and DSC.
   ➢ We agree with Reviewer 2 and we have reorganized the manuscript accordingly.

6.   In order to greatly improve the impact of the presented data, TGA studies in an oxidative environment is highly encouraged. Was this considered? It is believed that it should accompany the TGA studies in nitrogen that were presented.
   ➢ We understand the question of Reviewer 2. We performed some TGA measurements under air, especially to assess the stability of the cured material at the temperature of the curing. For PhBMI thermoset, there is no residual mass at 900°C as expected. Td5% has been measured at 365 °C which is roughly the same value than under nitrogen. For SiBMI thermoset, residual mass at 900 °C is 12% which is slightly lower than under nitrogen, because degradation of Si-containing polymers under oxidative conditions produces ceramic type residues, explaining the difference with carbon-based polymers. Td5% has been measured at 340 °C which is also lower than under nitrogen (40 °C of difference). TGA thermograms under air are presented below.

However, we did not include the analyses in the manuscript because we believe these data are not relevant regarding the application of those kinds of polymers. Polymers for thermal protection systems are studied by TGA under inert atmosphere in order to assess thermal stability under pyrolysis conditions, for thermal protection system applications. For example, Torre et al. explain in their paper that "Thermal analysis experiments have been performed in a nitrogen atmosphere (200 cm^3 min^{-1}), simulating the non-oxidative conditions occurring at the surface of the ablator." https://link.springer.com/article/10.1023/A:1004399923891. This paper is the first of a series about the characterization of materials for Thermal Protection Systems used in aerospace applications. Moreover, including TGA under air would have implied to perform degradation kinetics with those data, but we believe that it would have given inconsistent results, due to more complex degradation pathways, as illustrated by the results for PhBMI Thermoset displayed here.
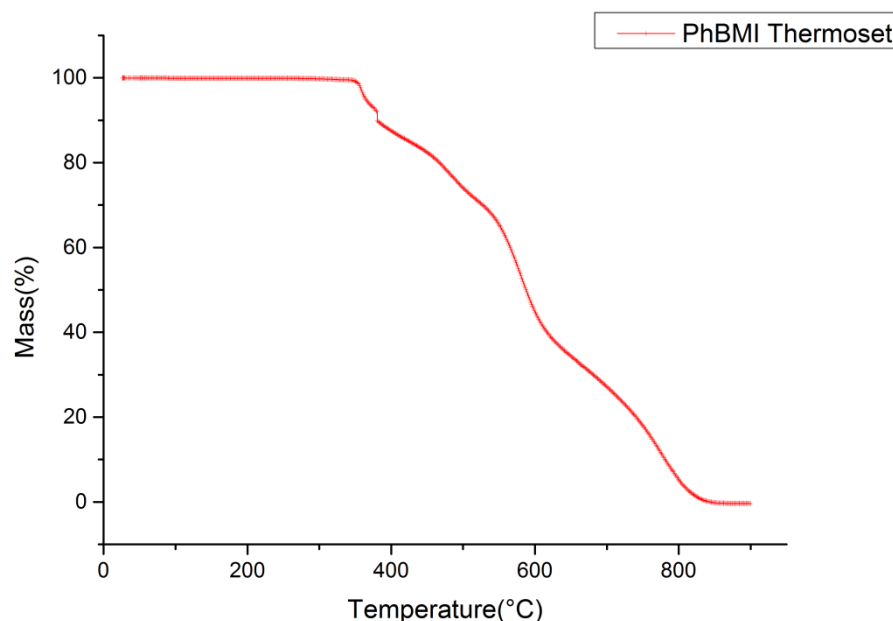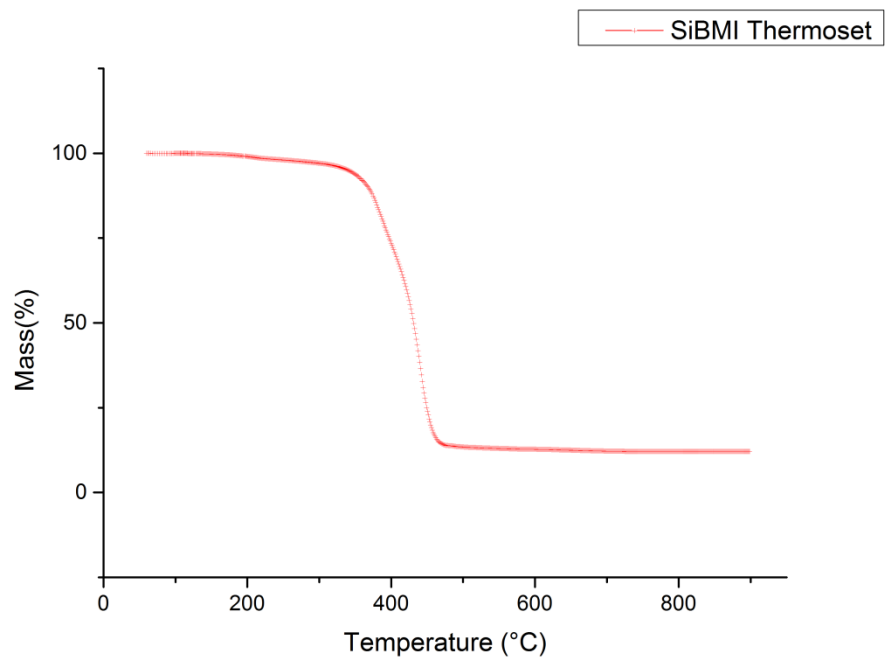
7.   The introduction is lacking key references from the field of high performance, bio-based thermosetting resins and composites, including work by La Scala, Gross, Stanzione, Palmese, Abu-Omar, and Dean Webster, and Bert Sels, to name a few. It is highly recommended to review the literature again for such works and include such references where appropriate.
   ➢ We fully agree with Reviewer 2 and we included more references about biobased thermosets in the introduction.

8.   No funding sources? No acknowledgements?
   ➢ We included a statement about funding and conflict of interests in the revised manuscript. There was no special financial support for this work.

I thank you very much for your kind attention in considering my paper.

Yours Sincerely,

Dr HDR Sylvain CAILLOL

Highlights

- Trieugenol phosphate monomer was synthesized (TEP)
- Alder-ene thermosets were synthesize by reaction with TEP and bismaleimides
- Flexible Alder-ene thermosets were synthesized for the first time
- Rigid and flexible materials exhibit excellent thermal properties
- Thermal degradation was elucidated

Eugenol-based thermally stable thermosets by Alder-Ene reaction: from synthesis to thermal degradation

Mélanie Decostanzi,[a†] Romain Tavernier,[a†] Gaëlle Fontaine,[b] Serge Bourbigot,[b] Claire Negrell,[a] Sylvain Caillol[a]*
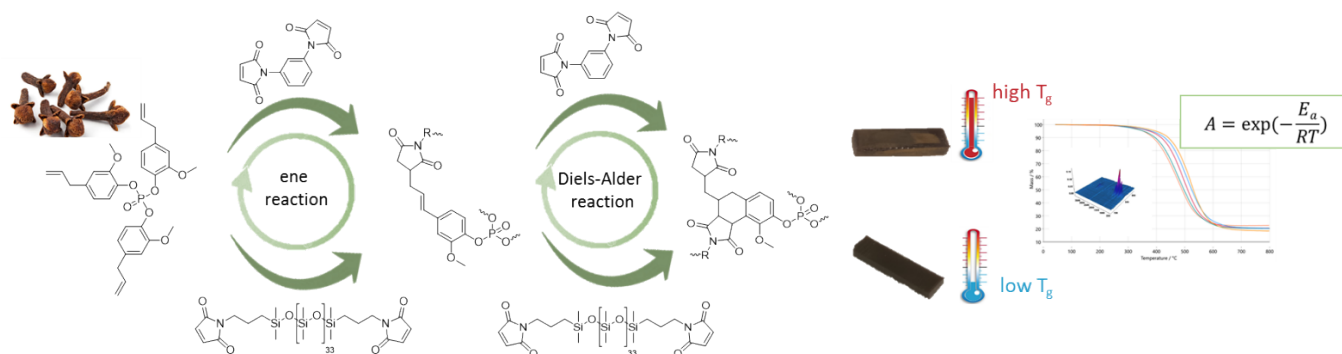
[a] ICGM, UMR 5253 – CNRS, Université de Montpellier, ENSCM, 240 Avenue Emile Jeanbrau 34296 Montpellier, France

[b] Univ. Lille, ENSCL, UMR 8207, UMET, Unité Matériaux et Transformations, 59000 Lille, France

[†] all authors have equally contributed

*Corresponding author: Sylvain Caillol, Email: sylvain.caillol@enscm.fr

Graphical Abstract

Abstract

Performing thermostable materials such as phenolic or epoxy networks are classically obtained from petrobased and harmful monomers. In this study, alternative solutions based on renewable eugenol trifunctional monomer (TEP) are proposed. Thus, innovative biobased Alder-ene thermosets are prepared by reacting TEP with two different bismaleimides : N,N'-1,3-phenylene bismaleimide (PhBMI) and polydimethylsiloxane bismaleimide (SiBMI) leading to different crosslinked aromatic networks. These materials exhibit various mechanical properties with very different T_g values of -113°C and 247°C for SiBMI and PhBMI materials respectively. However, both thermosets exhibit excellent thermal properties with elevated degradation temperature and high char yield. The degradation behavior was studied using thermogravimetric analysis – Fourier transformed infrared spectroscopy (TGA-FTIR): only

silicon compounds were observed for SiBMI, whereas phosphorus and carbonaceous products had specific signatures in degradation gases for PhBMI. Kinetic analysis of degradation confirmed those different behaviors. Our contribution with two original Alder-ene thermosets is an innovative way to develop sustainable versatile high-performant materials.

Keywords

Biobased; Alder-ene; eugenol; thermal properties; maleimide; thermoset

Introduction

Research on high performance thermosets is still a strong trend in polymer community, mainly because the targeted applications correspond to high value-added markets, such as aeronautics or aerospace industry. High performance is mainly achieved by generating high thermal stabilities and/or high glass transition temperatures, which can be obtained from high crosslinking densities and elevated aromatic content. Bismaleimides (BMIs) are curable polyimides and can be used to prepare high performance thermosets with superior mechanical and electrical properties, excellent physical property retention at elevated temperatures, thermal stability, low cost, and good processability.[1–3] However, BMIs are well known to give brittle materials because of their high aromaticity and their high crosslink density. To avoid this drawback, BMI can be blended with elastomers or be reacted with different chemical functions (*i.e* cyanate or allyl).[4–7] Thus, Alder-ene thermosets, which are a class of maleimide thermosets cured with olefinic compounds, such as allyl compounds, allow to reduce brittleness of BMI thermosets without weakening their heat resistance and good processing characteristics.[8][9] Maleimide moiety reacts through an ene reaction with allyl moiety, and another maleimide undergoes Diels-Alder cycloaddition on the newly formed double bond.[10] This curing behavior generates high crosslink densities resulting in high thermal performance materials.[11]

Alder-ene processes have also been used in order to improve properties of phenolics. For example allylation of the phenol moiety in novolacs, and subsequent cure reaction with bismaleimide, or functionalization of the phenolic polymers by both allyl and maleimide moiety result in Phenol-Maleimidophenol-Allylphenol-Formaldehyde thermosets.[4,12] This leads to complex curing processes involving both polycondensation and polyaddition.[13,14] Simple systems containing allylphenols and bismaleimides have also been investigated. Allylated bisphenol A, both on the

phenolic ring or on the hydroxyl group, has been widely used in combination with different bismaleimides to yield such thermosets.[4,9,15–17]

The use of biobased chemicals is also an important area of polymer research, in order to lower the environmental impacts of resulting materials, or to overcome fossil resource depletion. Moreover, investigation on new biobased molecules for polymers with new properties is also gaining increasing interest, especially in thermosets field.[18] Several studies have been conducted on the synthesis and polymerization of aromatic biobased monomers, in order to obtain thermosetting materials with enhanced properties, for example using vanillin,[19,20] or other lignin derivatives,[21–24] cardanol,[25] other plant oils and carbohydrates[26], cellulose derivatives[27] or tannins.[28] Eugenol, an allyl natural phenol easily extracted from cloves, is of prime interest for BMI chemistry, indeed it is used for the synthesis of BMI thermosets.[29] Eugenol-based monomers can be cured with bismaleimides, resulting in materials with very interesting performances, such as high char yields. Such high thermal stability is sometimes difficult to obtain with biobased materials, due to their higher oxygen content or lower aromatic density compare to petrobased chemicals.[30,31] It has been shown that the use of monomers containing several eugenol units is interesting for the generation of strong thermal properties. In a previous study, we also showed that the use of a phosphorus containing monomer synthesized with three eugenol residues led to the enhancement of the stability of epoxy thermosets,[32] which has been confirmed in a following study investigating flame retardancy properties.[33] Moreover, it has been showed that the use of a phosphorus-containing allylated monomer can enhance the properties of BMI thermosets.[34] Recently, it has been shown that an eugenol-based phosphate is a suitable monomer for the synthesis of bismaleimide thermosets with flame retardant properties.[35]

Alder-ene chemistry is still widely used to improve BMI thermoset properties, but the tuning of the properties of those thermosets is usually achieved by the synthesis of functional allylated monomers.[12,16,36–38] In this study, we used trieugenol phosphate, which we previsouly reported, with two different bismaleimides in order to synthesize novel Alder-ene thermosets and to evaluate the influence of the bismaleimide structure on the performances and degradation behavior of the obtained materials. In one hand, we used a commercially available aromatic bismaleimide, the *N,N'*-1,3-phenylene bismaleimide (PhBMI), in order to obtain high T_g material, and on the other hand, we synthesized a new polydimethylsiloxane-containing bismaleimide (SiBMI), resulting in a very low T_g

material. We analyzed the thermo-mechanical properties and studied the degradation of those thermosets.

Materials and methods

    1) Materials

Poly(dimethylsiloxane), bis(3-aminopropyl) terminated $(\overline{Mn} = 2{,}500 \text{ g/mol})$ (PDMS-amine) was purchased from ABCR, *N,N'*-1,3-phenylene bismaleimide (97 %), Zinc dichloride (98 %), Hexamethyldisilazane (>97 %), eugenol (99 %), phosphorus oxychloride (99 %) and triethylamine (99 %) were supplied by Sigma-Aldrich and were used without purification. Deuterated solvent $CDCl_3$ was obtained from Eurisotop for NMR study. Dichloromethane and toluene were purchased from VWR and used as received.

    2) Methods

NMR Analyses: Proton and carbon nuclear magnetic resonance (^{1}H and ^{13}C NMR) analyses were performed in deuterated chloroform ($CDCl_3$) using a Bruker Advance 400 MHz NMR spectrometer at a temperature of 25 °C. NMR samples were prepared as follows: 10 mg of product for ^{1}H experiment in around 0.4 mL of $CDCl_3$. The chemical shifts were reported in part per million. Spin multiplicity is shown by s = singlet, d = doublet, t = triplet, m = multiplet.

Infrared spectroscopy, for thermoset characterization **:** Attenuated Total Refraction Infrared spectra were recorded on a Nicolet 210 Fourier transform infrared spectroscopy (FTIR) spectrometer with a resolution of 4 cm^{-1}. The characteristic IR absorptions mentioned in the text are reported in cm^{-1}.

Thermogravimetric analyses (TGA), for char determination, were performed using a Netzsch TG 209F1 at a heating rate of 10 °C/min. Approximately 10 mg of monolitic sample was placed in an alumina crucible and heated from room temperature to 900 °C under nitrogen atmosphere (40 mL/min). Nitrogen atomosphere is used in order to reproduce pyrolysis conditions, allowing the formation of char, as described in literature[39].

Thermogravimetric coupled with Fourier-transform infrared (TG-FTIR) analyses, for volatiles characterizations, were performed using a TA Instruments Discovery TGA coupled with Thermo Fischer Nicolet IS10. After a 2 hours isotherm at 40 °C under nitrogen, a heating rate of 10 °C/min was applied until 800 °C. FTIR was performed during the heating ramp, from 4000 to 400 cm^{-1} with a resolution of 4 cm^{-1} (8 scans every 11 s).

Thermogravimetric analyses for degradation kinetics were carried out using a Netzsch TG 209 F1 Libra at five heating rates (1, 2, 5, 10 and 20 °C/min) from 30°C to 800 °C in nitrogen flow (50 mL/min). Samples of exactly 10 mg ($\pm$ 0.3 mg) were put in open alumina pans. Note that according to the good practice of TGA, it can be reasonably assumed at this mass and at those selected heating rates, the

samples can be considered as thermally thin. Typically, two replicates were run for each sample, and the average was reported. Both the onset (5% mass fraction loss) and peak mass loss rate have an uncertainty of 0.9°C (2σ). We corrected for each heating rate the buoyancy force (calibration with empty pan). Kinetic analysis and modeling of the degradation of the samples was made using an advanced thermokinetic software package (Kinetics Neo) developed by Netzsch Company.[40] For kinetic analysis, it is assumed that the material decomposes according to the Equation 1:

$$A_{solid} \rightarrow B_{solid\ or\ liquid} + C_{gas}$$

Equation 1

The rate expression $d\alpha/dt$, where α is the degree of conversion, is assumed to be defined by Equation 2:

$$d\alpha/dt = k(T).f(\alpha)$$

Equation 2

where k is the kinetic constant, $k = A.exp(-E/RT)$ according to the Arrhenius law, A is the frequency factor, E is the activation energy and $f(\alpha)$ is the so-called "reaction model". All reactions are assumed to be irreversible. In the case of decomposition and since the evolved gases were continuously removed by the fluid flow in the TGA chamber, this is a reasonable assumption. It is also assumed that the overall reaction (Equation 1) is the sum of individual reaction steps (formal or true step) with constant activation energy, as generally accepted in chemistry. The model can then include competitive, independent and successive reactions. The equations were solved with multivariate kinetic analysis (determination of the parameter via an hybrid regularized Gauss-Newton method or Marquardt method).

Differential scanning calorimetry (DSC) analyses were carried out using a NETZSCH DSC200F3 calorimeter. Constant calibration was performed using indium, *n*-octadecane and *n*-octane standards. Nitrogen was used as the purge gas. Approximately 10 mg of monolithic sample were placed in pierced aluminum pans and the thermal properties were recorded between -150 °C and 150 °C for the PDMS-amine based material and from 20 °C to 300 °C for the other materials at 20 °C/min to observe the glass transition temperature. The T_g values were measured during the second heating ramp to remove the thermal history of the polymer. All the reported temperatures are averaged values of 3 T_g determinations during the same analysis, with uncertainty presented using one standard deviation (1 σ).

Dynamic Mechanical Analyses (DMA) were carried out on Metravib DMA 25 with Dynatest 6.8 software. Uniaxial stretching of samples was performed while heating at a rate of 3 °C/min from ≈ T_g - 125 °C to T_g 25 °C for SiBMI-based material and from 30 °C to 320 °C for PhBMI-based material, keeping frequency at 1 Hz with a fixed strain of 10^{-5} m. This dynamical strain has been chosen to keep the material on its elastic domain with reversible mechanical stress. All sample were dimensioned according to specification from Metravib, respecting ISO6721.4 standard. PhBMI Thermoset sample was 9 mm×8.34 mm×3.4 mm (height×width×thickness) and SiBMI was 12 mm×4.4 mm×2.1 mm.

Swelling index: Three samples of around 30 mg each were separately put in THF for 24 h. The swelling index (SI) was calculated using the Equation 3 where m_1 is the mass of the material after swelling in THF and m_2 is the initial mass of the material.

$$Equation\ 3 \qquad SI = \frac{m_1 - m_2}{m_2} \times 100$$

Gel content: After SI measurements, the three samples were dried in a ventilated oven at 70 °C for 24 h. The gel content (GC) was calculated using the Equation 4, where m_3 is the mass of the material after the oven and m_2 is the initial mass of the material.

$$Equation\ 4 \qquad GC = \frac{m_3}{m_2} \times 100$$

3) Monomers/Polymers syntheses

   a. Synthesis of monomers

      i. Trieugenylphosphate (TEP) and *N,N'*-1,3-phenylene bismaleimide (PhBMI)

Trieugenylphosphate monomer has been synthesized according to our previsou reported work,[32] and is abbreviated TEP. *N,N'*-1,3-phenylene bismaleimide is commercially available and was used as received, and is abbreviated PhBMI in this article.

      ii. Synthesis of new PDMS-containing bismaleimide (SiBMI)

PDMS-based bismaleimide is a linear maleimide terminated polydimethylsiloxane, abbreviated SiBMI. It was synthesized according to the following procedure, adapted from the literature:[41] Maleic anhydride (4.66 g, 47.5 mmol) was dissolved in 100 mL of dichloromethane (DCM) in a 250 mL round-bottom flask. Then a solution of 20 g (8 mmol) of poly(dimethylsiloxane), bis(3-aminopropyl) terminated ($\overline{Mn} = 2,500$ g/mol) (PDMS-amine) in 40 mL of DCM was added dropwise to the maleic anhydride solution, at ambient temperature, and stirred for 1h. Then, solvent was removed under reduced pressure. The isolated mixture was dissolved in 100 mL of toluene. Then, zinc dichloride (6.5 g, 47.7 mmol) and hexamethyldisilazane (7.6 g, 47.1 mmol) were added to the solution, and heated at

80°C for 5h. The resulting mixture was filtered, and the solvent was removed under reduced pressure to afford the desired product. ^{1}H NMR (CDCl$_3$): δ = 0.10 (m, 237.5 H, CH$_3$Si), 0.50-0.55 (m, 5.4 H, CH$_2$Si), 1.60-1.64 (m, 5.3 H, CH$_2$CH$_2$CH$_2$), 3.52 (t, J = 7.2 Hz, 4.7 H, NCH$_2$), 6.71 (s, 4 H, HC=CH).

b. Polymers synthesis

In order to obtain homogeneous mixtures, monomers have been mixed under vacuum with a Speedmixer DAC 400.2 VAC-P for 5 min at 2500 rpm.

i. Curing of TEP/PhBMI system

A mixture of 2.2 g (4.1 mmol) of TEP and 1.8 g (6.7 mmol) of PhBMI (1 eq of allyl function per eq of maleimide function) has been poured in small PTFE molds. Samples have been cured under vacuum in order to remove air bubbles. A slow curing program with a low temperature ramp (1h at 50 °C, 1h at 80 °C, 1h at 100 °C, 1h at 120 °C, 1h at 150 °C and 180°C overnight) have been chosen instead of a high temperature isotherm curing (200°C) since the latter results in the trapping of air bubbles, which did not happen with the slow program. The resulting cured material appeared as a very hard transparent brown to yellow material.

ii. Curing of TEP/SiBMI system

A mixture of 200 mg (0.37 mmol) of TEP and 2 g (0.75 mmol) of SiBMI (1 eq. of allyl function per eq of maleimide function) was poured into a rectangle silicone mold. The sample has been cured at 180 °C for 24 hours. We obtained a smooth dark brown material.
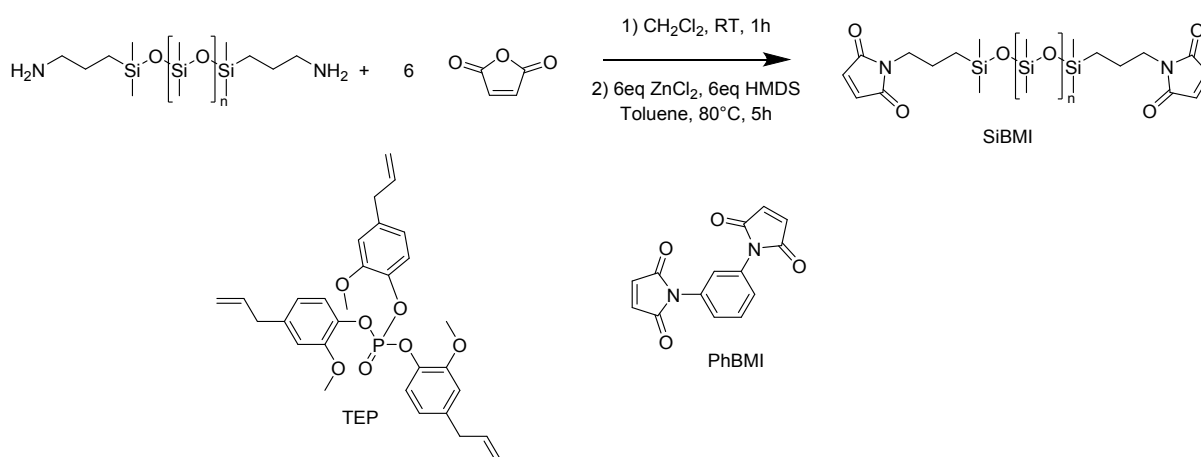

Figure 1 : Pictures of the cured materials.

Results and discussion

1) Description of monomers, synthesis and characterization of the new PDMS-containing bismaleimide

A trifunctional monomer is obtained using a phosphate group, substituted by three eugenol moieties. Thus, the triallyl monomer (trieugenylphosphate) has been synthesized according to our previous work.[32] It shall be noted that this synthesis has also been described using water as the solvent.[42] In addition, another advantage of this phosphorus containing triallyl monomer is that phosphate promotes charring and stabilizes char from oxidation. The commercially available bismaleimide is composed of a six-membered aromatic ring with two maleimide moieties in 1,3 positions. The PDMS containing bismaleimide (SiBMI) has been synthesized by reaction of a commercially available PDMS diamine (with a molar mass of 2,500 g/mol) with maleic anhydride (Scheme 1). In Figure 2 are presented ^{1}H NMR spectra of maleic anhydride, PDMS-diamine and synthesized PDMS bismaleimide. In the ^{1}H NMR spectrum of SiBMI (Figure 2, blue spectrum), the singlet *e* at 6.71 ppm has been assigned to newly formed maleimide double bond protons, and we can observe that the e" singlet at 7.04 ppm from the maleic anhydride has disappeared in the BMI spectrum. Triplet *d* at 3.52 ppm is assigned to methylene protons in the alpha position of the amine moiety. The shift of the protons from the amine *d"* in the red spectrum can be observed, which confirms the addition to the anhydride. Multiplet *c* around 1.60 ppm is assigned to middle methylene of the aminopropyl residue and 0.55-0.50 ppm multiplet signal *b* is assigned to the methylene in alpha position of the PDMS chain. The intense signal *a* at 0.10 ppm is assigned to the methyl protons of the polydimethylsiloxane chain. These attributions confirm that the corresponding maleimide is formed, and that no amine or anhydride is present in the product.

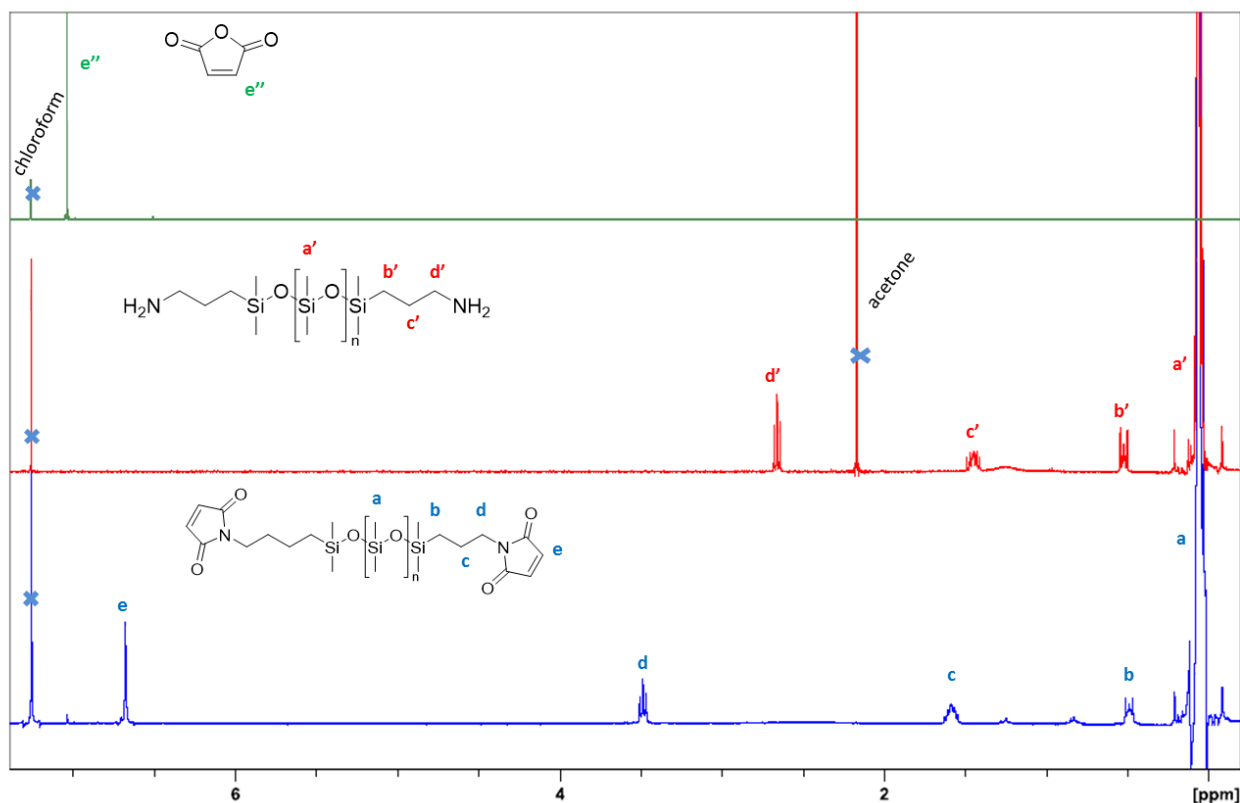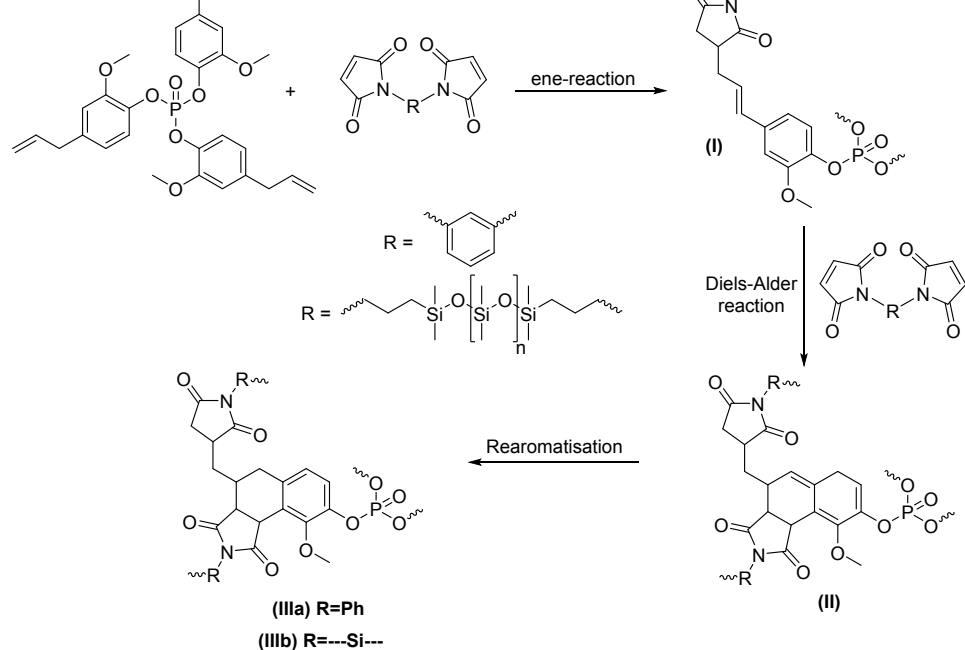*Scheme 1 : Synthesis of SiBMI and chemical structures of TEP and PhBMI.*

Figure 2: Stacked ^1H NMR spectra of maleic anhydride (top), PDMS-diamine (middle) and PDMS bismaleimide (bottom).

2) Characterization and properties of thermosets

The trifunctional allyl monomer (TEP) has been reacted with both bismaleimides: the aromatic one (PhBMI) and the PMDS-based one (SiBMI) following the synthetic pathway shown in Scheme 2. Firstly, an ene reaction is performed to obtain compound (I) containing intern unsaturation which acts as a diene in a Diels-Alder (DA) reaction. Hence, the maleimide moiety acting as a dienophile in DA reaction, reacts with (I) to form the intermediate (II). Then, a thermal re-aromatization takes place to form the aromatic species (III). These reactions led, if an aromatic bismaleimide is used, to a rigid thermoset (IIIa) due to the presence of many aromatic moieties. On the contrary, the use of a silicon-based bismaleimide led to a flexible material (IIIb) with low glass transition temperature.

Since all these reactions occur during the formation of the thermosets, the curing temperature is crucial. In fact, the homopolymerization takes place at high temperature and consumes the maleimide function.[9] Furthermore, the aromatic bismaleimide is hard to process because it is a solid compound. A slow raise of the temperature up to 200 °C under vaccum was performed to avoid the formation of

bubbles in the thermoset, and it was kept overnight at that temperature and under vacuum. In the case of the use of the PDMS-bismaleimide, which is liquid, these precautions were not necessary and the temperature was only kept constant at 200 °C for 24 hours. Bulk materials have been molded in order to perform thermal and physico-mechanical tests.

Scheme 2 : Synthetic pathway for the formation of thermosets.

An infrared analysis was performed to characterize the thermosets. The spectra were compared to those of TEP monomer and bismaleimide compounds. Figure 3 shows the comparison between the TEP monomer, the PhBMI and the corresponding obtained thermosets (IIIa).

In Figure 3, the absorption bands associated with the unsaturation of allyl function (1444 and 976 cm^{-1}) decreased and the one of the unsaturation of the maleimide (867 cm^{-1}) totally disappeared.[15] In the spectrum IIIa, different characteristic bands appeared. The band at 952 cm^{-1} can be assigned to the stretching vibration of the intermediate trans-olefinic product coming only from the ene-reaction (Scheme 2-(I)).[43] In fact, if the intermediate (II) were isolated, an absorption band between 790 and 840 cm^{-1} should be observed. Thus, this intermediate immediately turns into thermal re-aromatization and is not observed. Many absorption bands, corresponding to the formation of C-C bonds, were observed (1155, 1270 and 1495 cm^{-1}) demonstrating that the Diels-Alder reaction was performed.

The IR spectrum of the PDMS thermoset was not relevant because the high intensity of the bands corresponding to the silicon moiety hides the other signals.
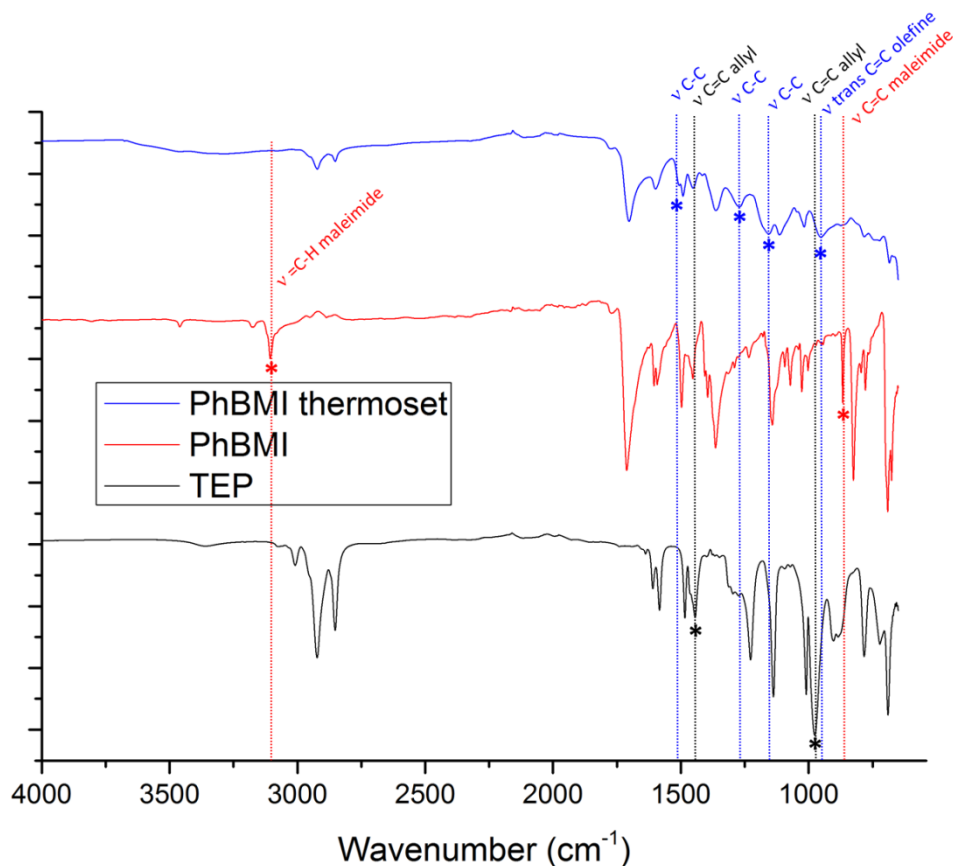
Figure 3 : Stacked infrared spectra of TEP (top), PhBMI (middle) and PhBMI thermoset (bottom).

The cross-linking degree of the network has been characterized with gel content (GC) and swelling index (SI) measurements (Table 1). Gel content corresponds to the residual mass of materials after immersion in THF. With value of 100%, cross-linking is complete for the PhBMI thermoset without any free species trapped in the network. The silicon material presents lower GC values corresponding to the presence of non fully reacted PDMS chains. Swelling index is an indication of the cross-linking density and the penetration of the solvent inside the material. The PhBMI thermoset exhibits the lowest swelling index. In fact, the cross-linking density of the SiBMI material is lower than the one of PhBMI thermoset due to high molar mass of the PDMS maleimide. Thus, the solvent has easier access into the SiBMI material.

Thermal measurements have been achieved to examine thermal properties of each material and are summarized in Table 1. TGA measurements were carried out under inert atmosphere to characterize thermal stability of the materials. The 5 %wt degradation occurred over 350 °C in both cases (Table 1). For the silicon thermoset IIIb, it is well-known that the Si-O bond confers a high thermal stability to the

material thanks to its high bond energy (796 kJ.mol^{-1}).[44] For the PhBMI thermoset IIIa, the high aromaticity content of the material also provides high thermal stability.[45] Furthermore, this high aromaticity entails high char yield (60 %) while a residual mass of 20 % was obtained when the silicon monomer was used. Actually, under an inert atmosphere, depolymerization of the PDMS occurred via the formation of volatile cyclic oligomers during the rupture of the Si-O bond.[46] Furthermore, the rupture of the Si-C bond allows the formation of ceramic silicon-oxycarbide which could lead to some residues. [47] In addition, the presence of phosphate moiety (*i.e* in TEP) in thermosets is well known to enhance char formation in pyrolysis conditions. [48,49]

Table 1 : Thermal and thermo-mechanical properties of materials

	Phosphate content (wt%)	Swelling Index (%)	Gel content (%)	T_g (°C)	$T_{d5\%}$ (°C)	Residual mass (%)	$T\alpha$ (°C)	E'glassy (GPa)	E'rubbery (MPa)
PhBMI thermoset IIIa	10.0	137	100	247 ± 3	359	60	275	1.49 ± 0.01	-
SiBMI thermoset IIIb	1.6	407	91	-113 ± 1	381	20	-114	-	4.4 ± 0.7

Thermo-mechanical properties of the two different materials have been compared by dynamical mechanical analysis (DMA) and the results are outlined in Table 1. The storage modulus (E') and tan δ as function of the temperature for both PhBMI and SiBMI thermosets are shown in Figure 4 and Figure 5 respectively. The alpha-transition temperatures have been measured at the maximum of the tan δ for each material. Tα values followed the same trend as T_g values measured by DSC. Narrow peak of tan δ for SiBMI-based materials shows a good homogeneity of the materials but the tan δ of PhBMI material exhibits a wide peak. This can be explained by the high aromaticity of the PhBMI thermoset which makes the diffusion of the monomers harder than in the SiBMI material. Thus, at room temperature the SiBMI thermoset is in its rubbery domain while the PhBMI material is in its glassy domain. Hence, at room temperature, the PhBMI thermoset is stiff (E'$_{glassy}$ = 1.49 ± 0.01 GPa) while the SiBMI thermoset is more flexible (E'$_{rubbery}$ = 4.4 ± 0.7 MPa).
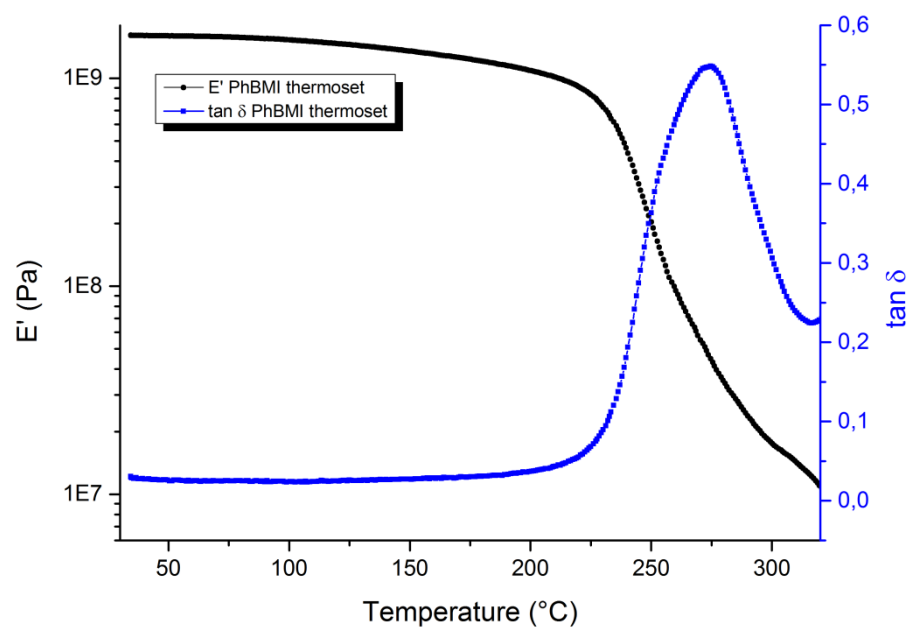
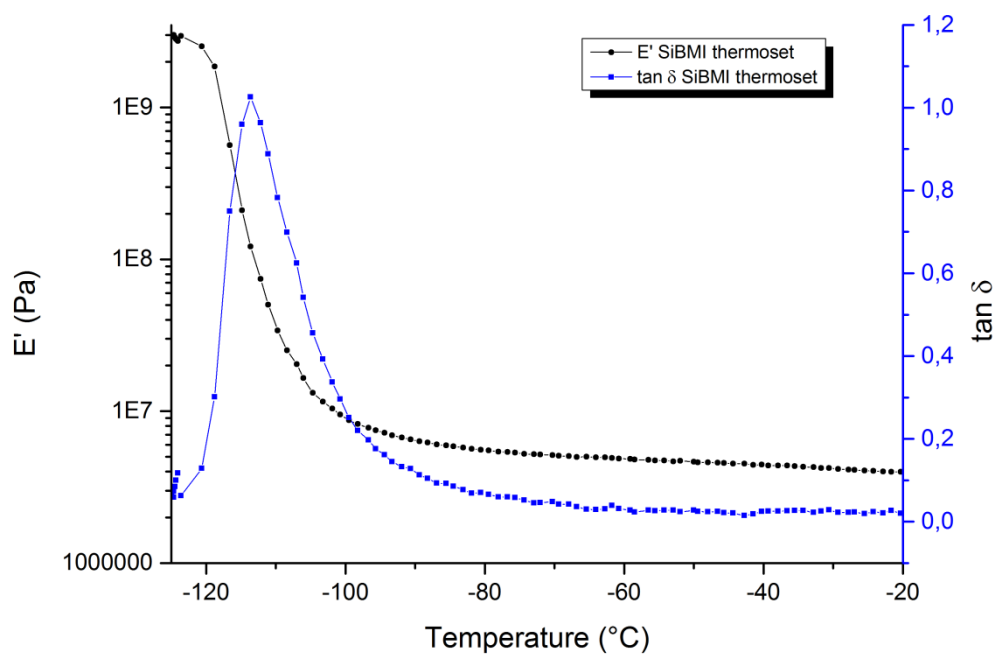*Figure 4: E' (dots) and tan δ (squares) of DMA curves for PhBMI thermoset.*

Figure 5 : E' (dots) and tan δ (squares) of DMA curves for SiBMI thermoset.

Finally, DSC measurements revealed a high glass transition temperature value (247 ± 3 °C) of the PhBMI material because of its high aromaticity content while a very low glass transition temperature (-113 ± 1 °C) was obtained with the SiBMI elastomer due to the presence of flexible segments.

3) Degradation behavior and kinetics analysis

It is known that phosphorus can act as a flame retardant in both gas and condensed phases.[50] TGA-FTIR has been performed in order to characterize the degradation products in pyrolysis conditions to gather data supporting the kinetic analysis discussed hereafter. 3D FTIR plots are presented in Figure 6 for both thermosets. Degradation of SiBMI thermoset shows an apparent single step decomposition occuring between 365 °C and 665 °C. Figure 7 shows the co-added FTIR spectra during this step and only decomposition products of the PDMS chains are detected: the 2969 cm^{-1} band is assigned to C-H bond vibration from the methyl moiety of PDMS, 1265 cm^{-1} band to C-H bond of $SiCH_3$, 1025 cm^{-1} band to Si-O-Si bonds and 815 cm^{-1} band to Si-O-C bonds. We can also observe at 3015 cm^{-1} a weak band corresponding to methane formed by a $Si-CH_3$ homolytic bond scission.[51] Degradation behavior of PhBMI thermoset is more complex, as shown by the TGA thermogram and FTIR analysis of volatiles (Figure 6-(a) and Figure 8). Until 340 °C, no volatiles are detected by FTIR. From 340 to 400 °C, a first significant weight loss is observed on TGA curve and broad bands at 2107 and 2178 cm^{-1} evidence the presence of CO. Hydrocarbons are also present with bands between 2800 and 3000 cm^{-1} and phosphorus-containing volatiles are detected, as shown by presence of bands at 1032 (P-O-C) and 1062 cm^{-1} (P=O) and as previously reported beforehands for bismaleimide-TEP thermoset.[35] Between 430 and 540 °C, CH_4 and CO are still observed, and CO_2 is detected by bands at 2309 and 2351 cm^{-1} and presence of methane is shown by sharp band at 3015 cm^{-1} in the IR spectrum. Between 730 and 800 °C, CO and CO_2 are detected. Water is present at all degradation stages and its signature is very intense starting from 340 °C: it avoids the detection of other degradation products due to the overlapping bands from water. We can conclude that PhBMI thermoset degradation products are mainly simple gases such as water, methane, carbone dioxide and monoxide, which is consistent with the fact that char yield is high. In addition, it is known that depending on the oxidation state of phosphorus in polymer matrix, volatiles observed by TGA-FTIR are different. Phosphates containing phenoxide moieties, such as in TEP, lead to an increased water release compared to phosphorus-containing building blocks without phenoxide. However, no phosphorus-containing compounds are detected when polymer matrix is an epoxy.[49,50] In our case no phosphorus in gas phase was observed in SiBMI thermoset whereas for PhBMI thermoset, some phosphorus species were observed in the early stage

of degradation. It shall be noted that for PhBMI thermoset, phosphate moiety (PO_4) represents nearly 10 wt% of the final material, whereas for SiBMI thermoset PO_4 represents only 1.6 wt%. Thus, phosphorus may not be detected in the case of SiBMI thermoset because of its very small amount. On the other hand, IR bands of silicon-containing volatiles may superpose to phosphorus-containing ones, in fact the SiBMI owns 77 wt% of silicon unit (Si-O-Me).
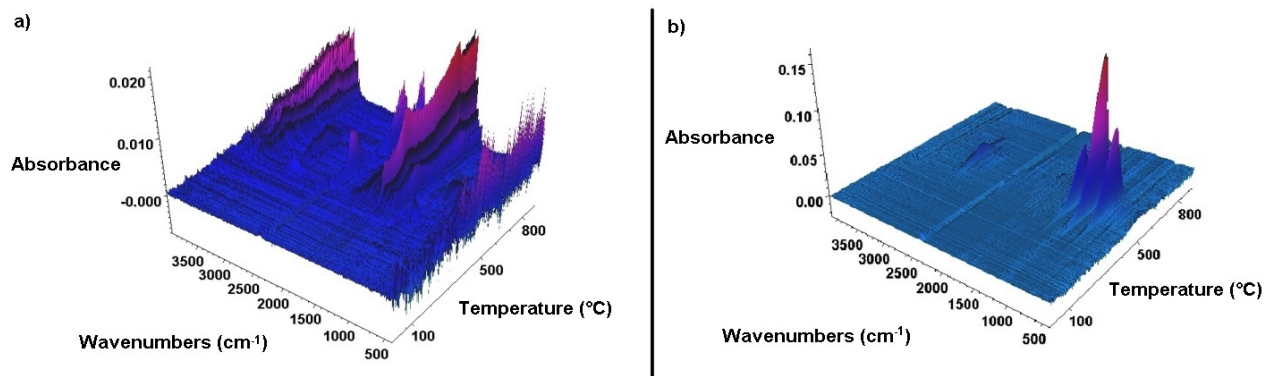

Figure 6 : 3D FTIR spectra of the volatiles products during TG analysis of PhBMI thermoset (a) and SiBMI thermoset (b)

Figure 7 : FTIR spectrum of SiBMI thermoset during TGA between 365 and 665 °C (coadded spectrum)
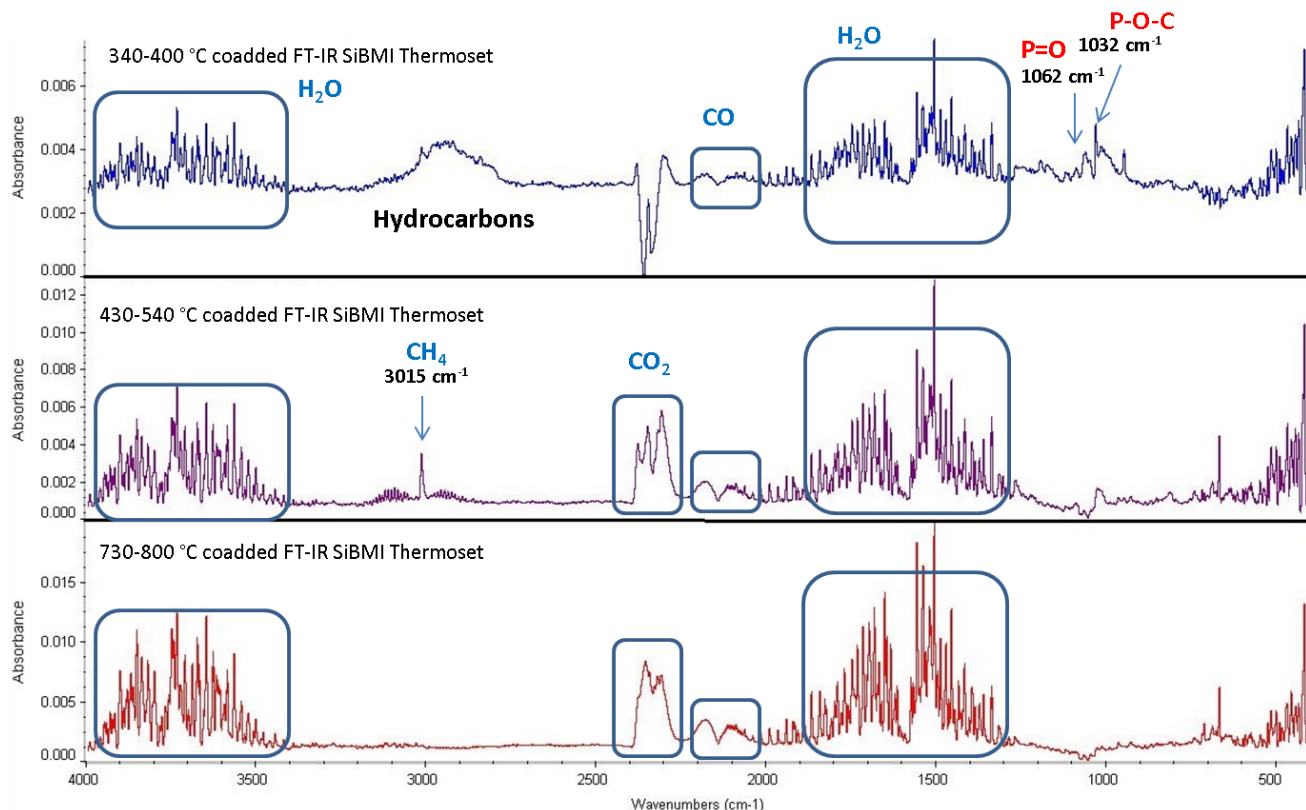
Figure 8 : FTIR spectrum of PhBMI thermoset during TGA at different stages of decomposition (coadded spectrum)

Kinetic analyses were performed on the thermal decomposition of the two thermosets (SiBMI and PhBMI thermosets) to get kinetic parameters, namely the triplet including the frequency factor (A), the activation energy (E) and the reaction order (n). Before starting any fitting procedure, it is necessary to define a model (combination of reactions) and to preset starting values for the kinetic parameters. A convenient approach is to use model-free analysis as a preliminary step of the kinetic analysis such as Friedman analysis.[52] A model-free analysis provides the plot of the activation energy versus the conversion degree. The two materials exhibit different behaviors. For SiBMi thermoset, the activation energy always increases as a function of conversion degree from 100 kJ/mol at low conversion degree to 450 kJ/mol at high conversion degree (Figure 9-(a)). On the other hand, the Friedman plot of PhBMI thermoset shows a plateau of activation energy about 620 kJ/mol up to a conversion degree of 0.8 and instability at higher conversion degree. The causes at the origin of those instabilities (PhBMI and SiBMI) can be multiple such as experimental and calculation system errors, thermal lag, temperature gradient, compensation effect, etc.[53] In the two cases, the Friedman plots indicate that the decomposition does not take place as a one-step reaction but as multi-step reactions.
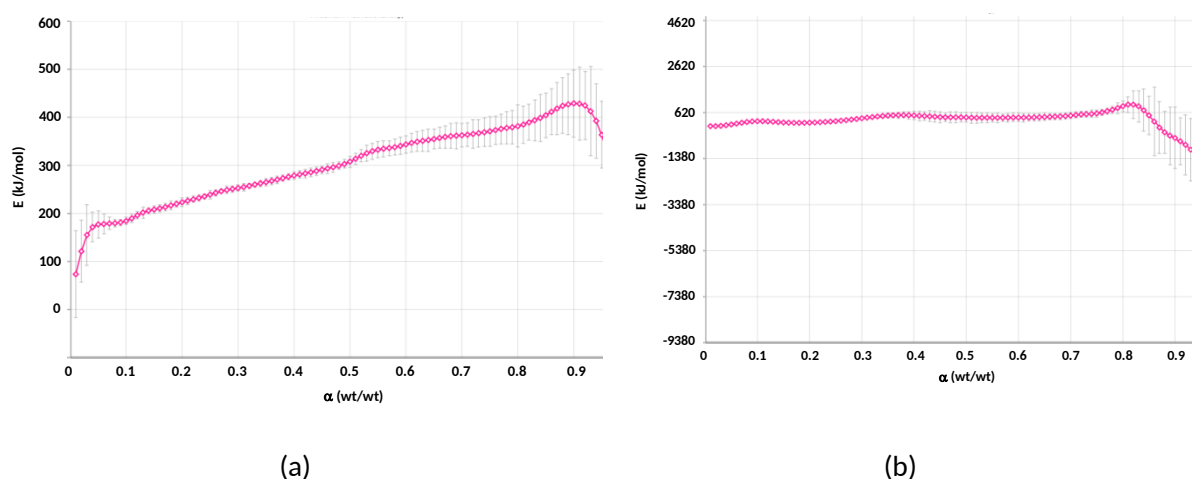
(a)   (b)

Figure 9 - Typical Friedman plots showing activation energies as a function of conversion degrees of (a) SiBMI thermoset and (b) PhBMI thermoset.

TG curve of SiBMI thermoset (Figure 10) shows an apparent single step of decomposition but the Friedman analysis suggested a multi-step decomposition. The simulation of the curves including only one single step does not give satisfactory results (result not shown). The combination of two successive reactions considering Avrami-Erofeev function gives a reasonable fit (Figure 11). The number of steps and the resulting calculated kinetic parameters (Table 2) are consistent with the values of activation energy calculated from the Friedman analysis. According to our modeling, the first step of decomposition contributes for 87 % and is therefore the main step of the decomposition of the SiBMI thermoset. According to TGA-FTIR analysis previously discussed, this step can be assigned to the decomposition of the PDMS chain contained in the thermoset. The calculated activation energy of 275 kJ/mol is consistent with a previous work on the kinetic analysis of the thermal decomposition of polysiloxane.[54] It was also reported that BMI-based thermoset decomposes in several steps with activation energy ranging between 150 and 350 kJ/mol, but no carbonaceous compounds were detected in FTIR.[55,56] The second step contributing at 13 % could be assigned to the species containing the maleimide ring.[57] It is consistent with the activation energy calculated at 400 kJ/mol, even if TGA-FTIR does not evidence this assumption. In SiBMI thermoset, nearly 77 % of the mass originates from the PDMS chains, so it is resonable to assume that some carbon or phosphorus-containing volatiles may not be detected. It has to be noted that this high value is also explained by the presence of phosphorus, due to high degradation bond energy compared to silicon or carbon-containing parts,[58] thus promoting char yield.
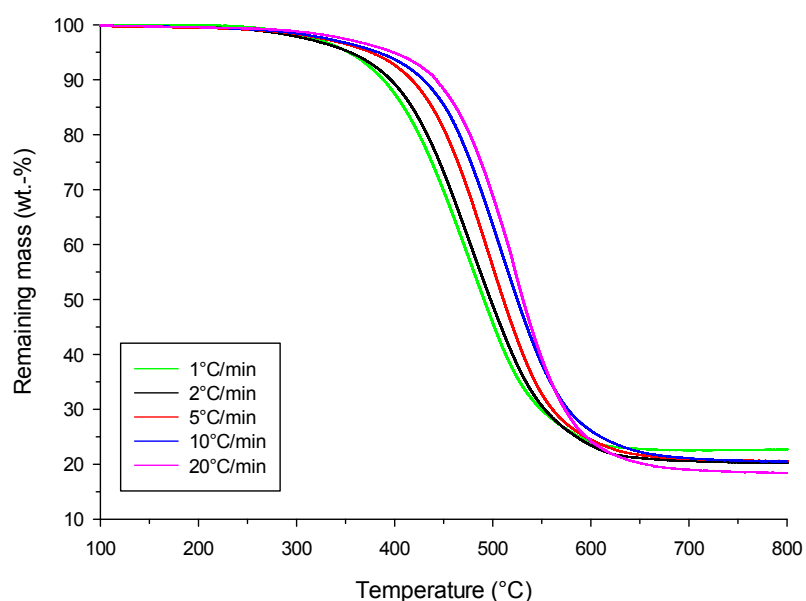
Figure 10 - TG curves of SiBMI thermoset as a function of heating rate (N2 flow)
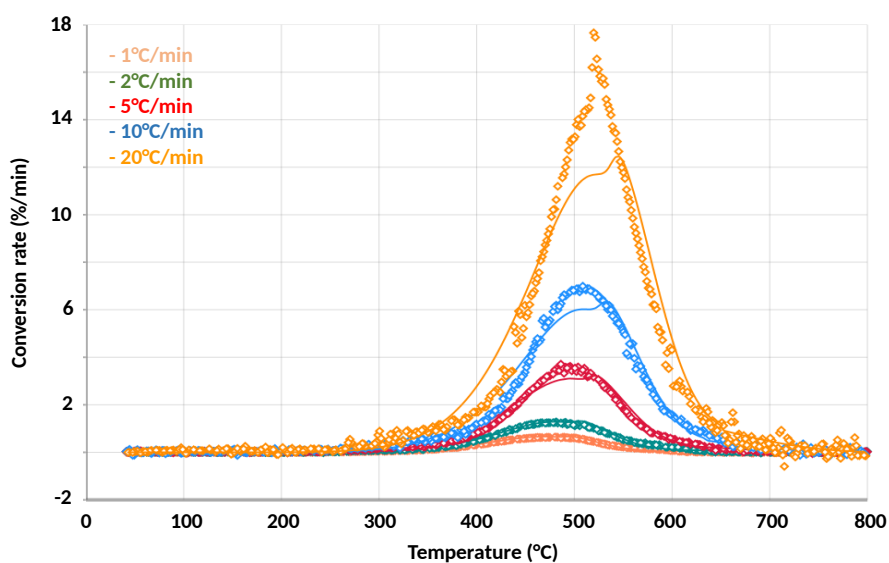

Figure 11 - Experimental and simulated DTG curves of SiBMI thermoset

TG curves of PhBMI thermoset (Figure 12) show a multi-step decomposition which seems more complex than that of SiBMI thermoset. The decomposition was simulated using three successive reactions considering Avrami-Erofeev reaction model (Figure 13). The fit cannot capture all the shape of the curve but it could not be improved using more complex reactional scheme or other reaction models. Table 2 shows the calculated kinetic parameters. The first step (16 %) is assigned to the

degradation of the methylene and allyl group in the structure as reported in literature.[59] It is consistent with TGA-FTIR evidencing the evolution of hydrocarbons and CO. It has to be noted that the activation energy is quite high because of the high number of crosslinks. The second step exhibits a much lower activation energy (128 kJ/mol vs. 281 kJ/mol) than the first step and its contribution is of 43 %. It corresponds to the decomposition of some maleimide part of the material and the volatilization of the remaining decomposed products.[59] Once again, TGA-FTIR supports this assignment showing the evolution of hydrocarbons, CO and CO_2. The third step, which contributes to 41 % of the decomposition, is assigned to the remaining maleimide rings as mentioned in the case of SiBMI thermoset. The activation energy is quite high (381 kJ/mol) and is similar to that of SiBMI thermoset. The reason for this high value is explained by the presence of phosphorus as mentioned above.
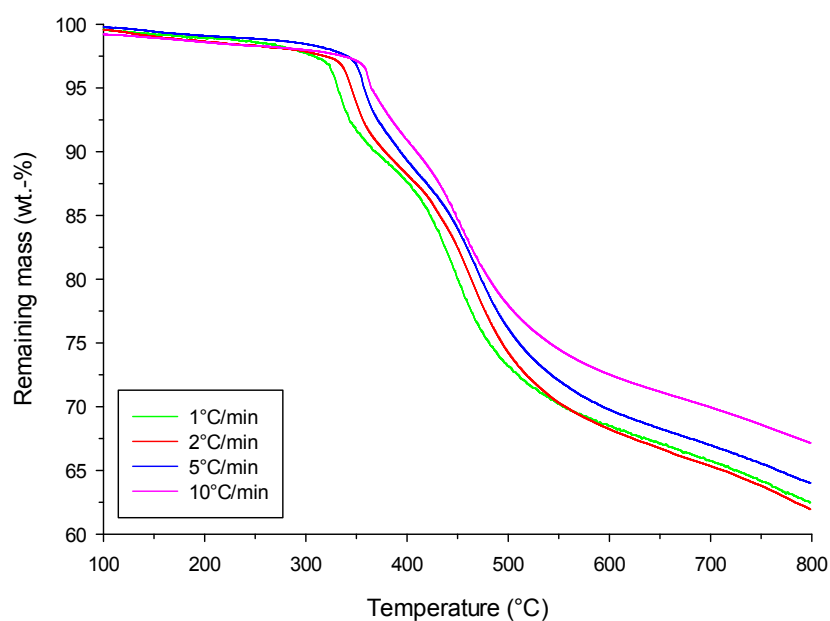

Figure 12 - TG curves of PhBMI thermoset as a function of heating rate (N_2 flow)
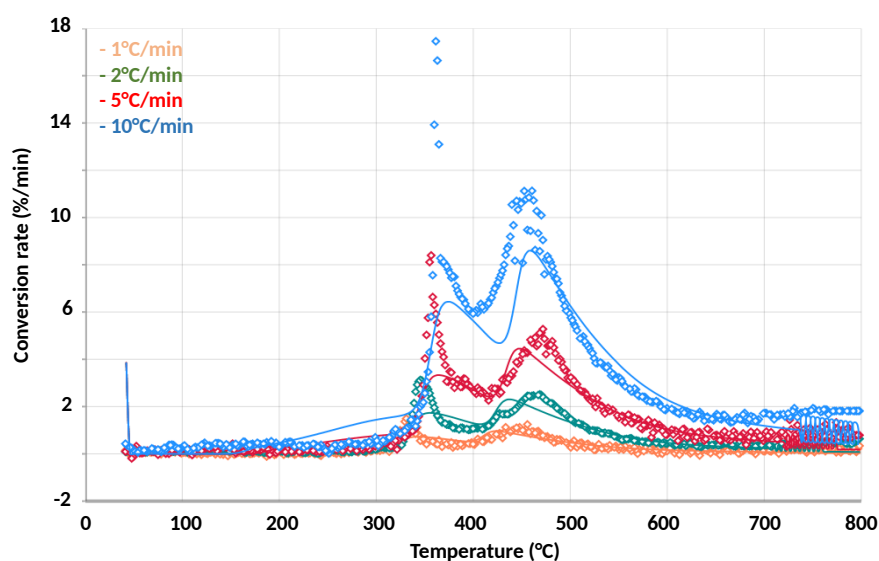
Figure 13 - Experimental and simulated DTG curves of PhBMI thermoset.

Table 2 - Computed kinetic parameters of the decomposition of SiBMI and PhBMI thermosets

Reaction N°	log(A) (A: s^{-1})	E (kJ/mol)	Dimension	Contribution to decomposition
SiBMI thermoset				
1	16 ± 0.9	275 ± 10	0.3 ± 0.1	87%
2	23 ± 1.8	400 ± 18	0.2 ± 0.1	13%
PhBMI thermoset				
1	22 ± 1.9	281 ± 12	0.2 ± 0.1	16%
2	7 ± 0.7	128 ± 8	0.1 ± 0.07	43%
3	25 ± 2.2	381 ± 17	0.1 ± 0.07	41%

Conclusion

Two Alder-ene thermosets were synthetized from renewable clove oil. Phosphate triallyl eugenol monomer was reacted with two types of bismaleimides with different structures: aromatic ring or PDMS oligomer, leading to two different Alder-ene thermosets, PhBMI or SiBMI respectively. Thus, these two bismaleimides lead to different thermally stable thermoset networks with various thermal and mechanical properties. The presence of PDMS chain in SiBMI gives a lower T$_g$ (around -113°C) and an important swelling due to the distance between to cross-linking nodes. In the contrary, aromatic

22

group of PhBMI increased strongly the rigidity of the material. Phosphate function improved the production of char for both Alder-ene thermosets with a char yield ranging from 20 % for SiBMI to more than 60% for PhBMI. Moreover, the degradation behaviors were studied by TGA-FTIR and kinetic analysis were made. The presence of silicon signal in the degradation gases for SiBMI did not make it possible to highlight the role of phosphorus in this material contrary to PhBMI. This latter one underwent multi-step degradation with higher total activation energy mainly due to the presence of phosphate function in the thermoset. The high properties of these new thermosets allowed to consider applications in highly demanding domains such as electronics, building or transport to replace toxic formo-phenolic resins.

Competing interest statement

The authors declare no competing interest.

Acknowledgements

References

[1]   X. Xiong, R. Ren, P. Chen, Q. Yu, J. Wang, C. Jia, Preparation and properties of modified bismaleimide resins based on phthalide-containing monomer, J. Appl. Polym. Sci. 130 (2013) 1084–1091. doi:10.1002/app.39269.

[2]   R.J. Iredale, C. Ward, I. Hamerton, Modern advances in bismaleimide resin technology: A 21st century perspective on the chemistry of addition polyimides, Prog. Polym. Sci. 69 (2017) 1–21. doi:10.1016/j.progpolymsci.2016.12.002.

[3]   H.D. Stenzenberger, Addition polyimides, in: High Perform. Polym., Springer-Verlag, Berlin/Heidelberg, n.d.: pp. 165–220. doi:10.1007/BFb0021199.

[4]   Y. Yan, X. Shi, J. Liu, T. Zhao, Y. Yu, Thermosetting resin system based on novolak and bismaleimide for resin-transfer molding, J. Appl. Polym. Sci. 83 (2002) 1651–1657. doi:10.1002/app.10073.

[5]   S. Takeda, H. Kakiuchi, Toughening bismaleimide resins by reactive liquid rubbers, J. Appl. Polym. Sci. 35 (1988) 1351–1366. doi:10.1002/app.1988.070350520.

[6]   A. Chaplin, I. Hamerton, H. Herman, A.K. Mudhar, S.J. Shaw, Studying water uptake effects in resins based on cyanate ester/bismaleimide blends☐, (2000) 12.

[7]   R.J. Iredale, C. Ward, I. Hamerton, Modern advances in bismaleimide resin technology: A 21st century perspective on the chemistry of addition polyimides, Prog. Polym. Sci. 69 (2017) 1–21. doi:10.1016/j.progpolymsci.2016.12.002.

[8]   M. Satheesh Chandran, C.P. Reghunadhan Nair, Maleimide-Based Alder-Enes, in: Handb. Thermoset Plast., Elsevier, 2014: pp. 459–510. doi:10.1016/B978-1-4557-3107-7.00012-9.

[9]   D. Reyx, I. Campistron, C. Caillaud, M. Villatte, A. Cavedon, Thermal reaction between N-phenylmaleimide and 2-allylphenol as a model for the crosslinking reaction in bismaleimide polymerization with diallylbisphenol A, Macromol. Chem. Phys. 196 (1995) 775–785. doi:10.1002/macp.1995.021960308.

[10]   I.D. Cunningham, A. Brownhill, I. Hamerton, B.J. Howlin, The ene reaction between maleimides and allyl-substituted aromatics, Tetrahedron. 53 (1997) 13473–13494. doi:10.1016/S0040-4020(97)00856-9.

[11]   H.D. SterLzenberger, T. GMBH-Verfahrenstechnik, Addition polyimides, (n.d.) 56.

[12]   C. Nair, Advances in addition-cure phenolic resins, Prog. Polym. Sci. 29 (2004) 401–498. doi:10.1016/j.progpolymsci.2004.01.004.

[13]   R.L. Bindu, C.P. Reghunadhan Nair, K.N. Ninan, Addition-cure-type phenolic resin based on alder-ene reaction: Synthesis and laminate composite properties, J. Appl. Polym. Sci. 80 (2001) 737–749. doi:10.1002/1097-4628(20010502)80:5<737::AID-APP1150>3.0.CO;2-V.

[14]   Z. Luo, L. Wei, F. Liu, T. Zhao, The effect of allylation degree on processing properties, thermal cure, and thermal properties of BMAN resins, J. Appl. Polym. Sci. 104 (2007) 2822–2829. doi:10.1002/app.25706.

[15]   J.C. Phelan, C.S.P. Sung, Cure Characterization in Bis(maleimide)/Diallylbisphenol A Resin by Fluorescence, FT-IR, and UV-Reflection Spectroscopy, Macromolecules. 30 (1997) 6845–6851. doi:10.1021/ma961887f.

[16]   A. Tiwari, A.K. Nema, C.K. Das, S.K. Nema, Thermal analysis of polysiloxanes, aromatic polyimide and their blends, Thermochim. Acta. 417 (2004) 133–142. doi:10.1016/j.tca.2003.10.003.

[17]   R.J. Morgan, E. Eugene Shin, B. Rosenberg, A. Jurek, Characterization of the cure reactions of bismaleimide composite matrices, Polymer (Guildf). 38 (1997) 639–646. doi:10.1016/S0032-3861(96)00542-3.

[18]   J.-M. Raquez, M. Deléglise, M.-F. Lacrampe, P. Krawczak, Thermosetting (bio)materials derived from renewable resources: A critical review, Prog. Polym. Sci. 35 (2010) 487–509. doi:10.1016/j.progpolymsci.2010.01.001.

[19]   M. Fache, B. Boutevin, S. Caillol, Vanillin, a key-intermediate of biobased polymers, Eur. Polym. J. 68 (2015) 488–502. doi:10.1016/j.eurpolymj.2015.03.050.

[20]   E.D. Hernandez, A.W. Bassett, J.M. Sadler, J.J. La Scala, J.F. Stanzione, Synthesis and Characterization of Bio-based Epoxy Resins Derived from Vanillyl Alcohol, ACS Sustain. Chem. Eng. 4 (2016) 4328–4339. doi:10.1021/acssuschemeng.6b00835.

[21]   E. Feghali, K.M. Torr, D.J. van de Pas, P. Ortiz, K. Vanbroekhoven, W. Eevers, R. Vendamme, Thermosetting Polymers from Lignin Model Compounds and Depolymerized Lignins, Top. Curr. Chem. 376 (2018). doi:10.1007/s41061-018-0211-6.

[22]   A. Llevot, E. Grau, S. Carlotti, S. Grelier, H. Cramail, From Lignin-derived Aromatic Compounds to Novel Biobased Polymers, Macromol. Rapid Commun. 37 (2016) 9–28. doi:10.1002/marc.201500474.

[23]   S. Zhao, M.M. Abu-Omar, Synthesis of Renewable Thermoset Polymers through Successive Lignin Modification Using Lignin-Derived Phenols, ACS Sustain. Chem. Eng. 5 (2017) 5059–5066. doi:10.1021/acssuschemeng.7b00440.

[24]   L. Yue, F. Liu, S. Mekala, A. Patel, R.A. Gross, I. Manas-Zloczower, High Performance Biobased Epoxy Nanocomposite Reinforced with a Bacterial Cellulose Nanofiber Network, ACS Sustain. Chem. Eng. 7 (2019) 5986–5992. doi:10.1021/acssuschemeng.8b06073.

[25]   S. Caillol, Cardanol: A promising building block for biobased polymers and additives, Curr. Opin.

Green Sustain. Chem. 14 (2018) 26–32. doi:10.1016/j.cogsc.2018.05.002.

[26]   X. Pan, D.C. Webster, New Biobased High Functionality Polyols and Their Use in Polyurethane Coatings, ChemSusChem. 5 (2012) 419–429. doi:10.1002/cssc.201100415.

[27]   F. Hu, J.J. La Scala, J.M. Sadler, G.R. Palmese, Synthesis and Characterization of Thermosetting Furan-Based Epoxy Systems, Macromolecules. 47 (2014) 3332–3342. doi:10.1021/ma500687t.

[28]   A. Arbenz, L. Avérous, Chemical modification of tannins to elaborate aromatic biobased macromolecular architectures, Green Chem. 17 (2015) 2626–2646. doi:10.1039/c5gc00282f.

[29]   D.G. Vassão, L.B. Davin, N.G. Lewis, Metabolic Engineering of Plant Allyl/Propenyl Phenol and Lignin Pathways: Future Potential for Biofuels/Bioenergy, Polymer Intermediates, and Specialty Chemicals?, in: Adv. Plant Biochem. Mol. Biol., 2008: pp. 385–428. doi:10.1016/S1755-0408(07)01013-2.

[30]   M. Shibata, N. Teramoto, T. Shimasaki, M. Ogihara, High-performance bio-based bismaleimide resins using succinic acid and eugenol, Polym. J. 43 (2011) 916–922. doi:10.1038/pj.2011.87.

[31]   M. Neda, K. Okinaga, M. Shibata, High-performance bio-based thermosetting resins based on bismaleimide and allyl-etherified eugenol derivatives, Mater. Chem. Phys. 148 (2014) 319–327. doi:10.1016/j.matchemphys.2014.07.050.

[32]   I. Faye, M. Decostanzi, Y. Ecochard, S. Caillol, Eugenol bio-based epoxy thermosets: from cloves to applied materials, Green Chem. 19 (2017) 5236–5242. doi:10.1039/C7GC02322G.

[33]   J.-T. Miao, L. Yuan, Q. Guan, G. Liang, A. Gu, Biobased epoxy resin derived from eugenol with excellent integrated performance and high renewable carbon content: Biobased epoxy resin derived from eugenol, Polym. Int. 67 (2018) 1194–1202. doi:10.1002/pi.5621.

[34]   S. Li, H. Yan, S. Feng, S. Niu, Synthesis and characterization of a phosphorus-containing flame retardant with double bonds and its application in bismaleimide resins, RSC Adv. 5 (2015) 101480–101486. doi:10.1039/C5RA15946F.

[35]   J.-T. Miao, L. Yuan, G. Liang, A. Gu, Biobased bismaleimide resins with high renewable carbon content, heat resistance and flame retardancy via a multi-functional phosphate from clove oil, Mater. Chem. Front. 3 (2019) 78–85. doi:10.1039/C8QM00443A.

[36]   X. Zhang, R. Akram, S. Zhang, H. Ma, Z. Wu, D. Wu, Hexa(eugenol)cyclotriphosphazene modified bismaleimide resins with unique thermal stability and flame retardancy, React. Funct. Polym. 113 (2017) 77–84. doi:10.1016/j.reactfunctpolym.2017.02.010.

[37]   A. Gu, Novel high performance RTM bismaleimide resin with low cure temperature for advanced composites, Polym. Adv. Technol. 16 (2005) 563–566. doi:10.1002/pat.615.

[38]   G. Liang, J. Fan, Novel modified bismaleimide resins with improved ablativity, J. Appl. Polym. Sci. 73 (1999) 1623–1631. doi:10.1002/(SICI)1097-4628(19990829)73:9<1623::AID-APP3>3.0.CO;2-Z.

[39]   L. Torre, J.M.M. Kenny, A.M. Maffezzoli, Degradation behaviour of a composite material for thermal protection systems Part I–Experimental characterization, J. Mater. Sci. 33 (1998) 3137–3143. doi:10.1023/A:1004399923891.

[40]   J. Opfermann, Kinetic analysis using multivariate non-linear regression. I. Basic concepts, J. Therm. Anal. Calorim. 60 (2000) 641–658. doi:10.1023/A:1010167626551.

[41]   T. Engel, G. Kickelbick, Furan-Modified Spherosilicates as Building Blocks for Self-Healing Materials: Furan-Modified Spherosilicates for Self-Healing Materials, Eur. J. Inorg. Chem. 2015 (2015) 1226–1232. doi:10.1002/ejic.201402551.

[42]   J.-T. Miao, L. Yuan, Q. Guan, G. Liang, A. Gu, Water-Phase Synthesis of a Biobased Allyl Compound for Building UV-Curable Flexible Thiol–Ene Polymer Networks with High Mechanical Strength and Transparency, ACS Sustain. Chem. Eng. 6 (2018) 7902–7909. doi:10.1021/acssuschemeng.8b01128.

[43]   G. Socrates, Infrared and Raman characteristic group frequencies: tables and charts, 3. ed, Wiley, Chichester, 2001.

[44]   S. Hamdani, C. Longuet, D. Perrin, J.-M. Lopez-cuesta, F. Ganachaud, Flame retardancy of silicone-based materials, Polym. Degrad. Stab. 94 (2009) 465–495. doi:10.1016/j.polymdegradstab.2008.11.019.

[45]   V.V. Korshak, V.A. Khomutov, Y.Y. Doroshenko, A study of thermal stability in a number of aromatic and nitrogen containing polycyclic compounds, Polym. Sci. U.S.S.R. 18 (1976) 597–603. doi:10.1016/0032-3950(76)90253-7.

[46]   T.H. Thomas, T.C. Kendrick, Thermal analysis of polydimethylsiloxanes. I. Thermal degradation in controlled atmospheres, J. Polym. Sci. Part A-2 Polym. Phys. 7 (1969) 537–549. doi:10.1002/pol.1969.160070308.

[47]   G. Camino, S.. Lomakin, M. Lageard, Thermal polydimethylsiloxane degradation. Part 2. The degradation mechanisms, Polymer (Guildf). 43 (2002) 2011–2015. doi:10.1016/S0032-3861(01)00785-6.

[48]   S. Bourbigot, S. Duquesne, Fire retardant polymers: recent developments and opportunities, J. Mater. Chem. 17 (2007) 2283. doi:10.1039/b702511d.

[49]   U. Braun, A.I. Balabanovich, B. Schartel, U. Knoll, J. Artner, M. Ciesielski, M. Döring, R. Perez, J.K.W. Sandler, V. Altstädt, T. Hoffmann, D. Pospiech, Influence of the oxidation state of phosphorus on the decomposition and fire behaviour of flame-retarded epoxy resin composites, Polymer (Guildf). 47 (2006) 8495–8508. doi:10.1016/j.polymer.2006.10.022.

[50]   B. Schartel, Phosphorus-based Flame Retardancy Mechanisms—Old Hat or a Starting Point for Future Development?, Materials (Basel). 3 (2010) 4710–4745. doi:10.3390/ma3104710.

[51]   G. Camino, S.. Lomakin, M. Lageard, Thermal polydimethylsiloxane degradation. Part 2. The degradation mechanisms, Polymer (Guildf). 43 (2002) 2011–2015. doi:10.1016/S0032-3861(01)00785-6.

[52]   H.L. Friedman, Kinetics of thermal degradation of char-forming plastics from thermogravimetry. Application to a phenolic plastic, J. Polym. Sci. Part C Polym. Symp. 6 (2007) 183–195. doi:10.1002/polc.5070060121.

[53]   M. Carrier, L. Auret, A. Bridgwater, J.H. Knoetze, Using Apparent Activation Energy as a Reactivity Criterion for Biomass Pyrolysis, Energy & Fuels. 30 (2016) 7834–7841. doi:10.1021/acs.energyfuels.6b00794.

[54]   G. Caminoa, S.M. Lomakin, M. Lazzari, Polydimethylsiloxane thermal degradation. Part 1. Kinetic aspects., Polymer (Guildf). 42 (2001) 2395–2402. doi:10.1016/0038-1101(90)90239-B.

[55]   C. Gouri, C.. Reghunadhan Nair, R. Ramaswamy, K.. Ninan, Thermal decomposition characteristics of Alder-ene adduct of diallyl bisphenol A novolac with bismaleimide: effect of stoichiometry, novolac molar mass and bismaleimide structure, Eur. Polym. J. 38 (2002) 503–510. doi:10.1016/S0014-3057(01)00197-5.

[56]   Q.-T. Pham, J.-M. Hsu, J.-P. Pan, T.-H. Wang, C.-S. Chern, Non-isothermal degradation kinetics of N , N ′-bismaleimide-4,4′-diphenylmethane/barbituric acid based polymers in the presence of hydroquinone, J. Appl. Polym. Sci. 130 (2013) 1923–1930. doi:10.1002/app.39360.

[57]   Q.-T. Pham, J.-M. Hsu, J.-P. Pan, T.-H. Wang, C.-S. Chern, Synthesis and characterization of phenylsiloxane-modified bismaleimide/barbituric acid-based polymers with 3-aminopropyltriethoxysilane as the coupling agent, Polym. Int. 62 (2012) n/a–n/a. doi:10.1002/pi.4390.

[58]   T. Ho, T. Leu, Y. Sun, J. Shieh, Thermal degradation kinetics and flame retardancy of phosphorus-containing dicyclopentadiene epoxy resins, Polym. Degrad. Stab. 91 (2006) 2347–2356. doi:10.1016/j.polymdegradstab.2006.04.002.

[59]   C. Gouri, C.. Reghunadhan Nair, R. Ramaswamy, K.. Ninan, Thermal decomposition characteristics of Alder-ene adduct of diallyl bisphenol A novolac with bismaleimide: effect of stoichiometry, novolac molar mass and bismaleimide structure, Eur. Polym. J. 38 (2002) 503–510. doi:10.1016/S0014-3057(01)00197-5.

Eugenol-based thermally stable thermosets by Alder-Ene reaction: from synthesis to thermal degradation

Mélanie Decostanzi,[a†] Romain Tavernier,[a†] Gaëlle Fontaine,[b] Serge Bourbigot,[b] Claire Negrell,[a] Sylvain Caillol[a]*
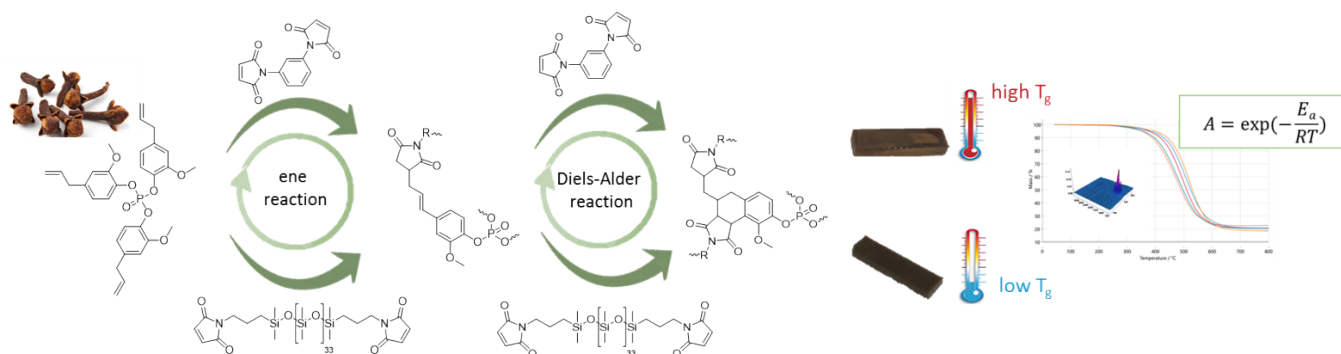
[a] ICGM, UMR 5253 – CNRS, Université de Montpellier, ENSCM, 240 Avenue Emile Jeanbrau 34296 Montpellier, France

[b] Univ. Lille, ENSCL, UMR 8207, UMET, Unité Matériaux et Transformations, 59000 Lille, France

[†] all authors have equally contributed

*Corresponding author: Sylvain Caillol, Email: sylvain.caillol@enscm.fr

Graphical Abstract

Abstract

Performing thermostable materials such as phenolic or epoxy networks are classically obtained from petrobased and harmful monomers. In this study, alternative solutions based on renewable eugenol trifunctional monomer (TEP) are proposed. Thus, innovative biobased Alder-ene thermosets are prepared by reacting TEP with two different bismaleimides : *N,N'*-1,3-phenylene bismaleimide (PhBMI) and polydimethylsiloxane bismaleimide (SiBMI) leading to different crosslinked aromatic networks. These materials exhibit various mechanical properties with very different T_g values of -113°C and 247°C for SiBMI and PhBMI materials respectively. However, both thermosets exhibit excellent thermal properties with elevated degradation temperature and high char yield. The degradation behavior was studied using thermogravimetric analysis – Fourier transformed infrared spectroscopy (TGA-FTIR): only

1

silicon compounds were observed for SiBMI, whereas phosphorus and carbonaceous products had specific signatures in degradation gases for PhBMI. Kinetic analysis of degradation confirmed those different behaviors. Our contribution with two original Alder-ene thermosets is an innovative way to develop sustainable versatile high-performant materials.

Keywords

Biobased; Alder-ene; eugenol; thermal properties; maleimide; thermoset

Introduction

Research on high performance thermosets is still a strong trend in polymer community, mainly because the targeted applications correspond to high value-added markets, such as aeronautics or aerospace industry. High performance is mainly achieved by generating high thermal stabilities and/or high glass transition temperatures, which can be obtained from high crosslinking densities and elevated aromatic content. Bismaleimides (BMIs) are curable polyimides and can be used to prepare high performance thermosets with superior mechanical and electrical properties, excellent physical property retention at elevated temperatures, thermal stability, low cost, and good processability.[1–3] However, BMIs are well known to give brittle materials because of their high aromaticity and their high crosslink density. To avoid this drawback, BMI can be blended with elastomers or be reacted with different chemical functions (*i.e* cyanate or allyl).[4–7] Thus, Alder-ene thermosets, which are a class of maleimide thermosets cured with olefinic compounds, such as allyl compounds, allow to reduce brittleness of BMI thermosets without weakening their heat resistance and good processing characteristics.[8][9] Maleimide moiety reacts through an ene reaction with allyl moiety, and another maleimide undergoes Diels-Alder cycloaddition on the newly formed double bond.[10] This curing behavior generates high crosslink densities resulting in high thermal performance materials.[11]

Alder-ene processes have also been used in order to improve properties of phenolics. For example allylation of the phenol moiety in novolacs, and subsequent cure reaction with bismaleimide, or functionalization of the phenolic polymers by both allyl and maleimide moiety result in Phenol-Maleimidophenol-Allylphenol-Formaldehyde thermosets.[4,12] This leads to complex curing processes involving both polycondensation and polyaddition.[13,14] Simple systems containing allylphenols and bismaleimides have also been investigated. Allylated bisphenol A, both on the

2

phenolic ring or on the hydroxyl group, has been widely used in combination with different bismaleimides to yield such thermosets.[4,9,15–17]

The use of biobased chemicals is also an important area of polymer research, in order to lower the environmental impacts of resulting materials, or to overcome fossil resource depletion. Moreover, investigation on new biobased molecules for polymers with new properties is also gaining increasing interest, especially in thermosets field.[18] Several studies have been conducted on the synthesis and polymerization of aromatic biobased monomers, in order to obtain thermosetting materials with enhanced properties, for example using vanillin,[19,20] or other lignin derivatives,[21–24] cardanol,[25] other plant oils and carbohydrates[26], cellulose derivatives[27] or tannins.[28] Eugenol, an allyl natural phenol easily extracted from cloves, is of prime interest for BMI chemistry, indeed it is used for the synthesis of BMI thermosets.[29] Eugenol-based monomers can be cured with bismaleimides, resulting in materials with very interesting performances, such as high char yields. Such high thermal stability is sometimes difficult to obtain with biobased materials, due to their higher oxygen content or lower aromatic density compare to petrobased chemicals.[30,31] It has been shown that the use of monomers containing several eugenol units is interesting for the generation of strong thermal properties. In a previous study, we also showed that the use of a phosphorus containing monomer synthesized with three eugenol residues led to the enhancement of the stability of epoxy thermosets,[32] which has been confirmed in a following study investigating flame retardancy properties.[33] Moreover, it has been showed that the use of a phosphorus-containing allylated monomer can enhance the properties of BMI thermosets.[34] Recently, it has been shown that an eugenol-based phosphate is a suitable monomer for the synthesis of bismaleimide thermosets with flame retardant properties.[35]

Alder-ene chemistry is still widely used to improve BMI thermoset properties, but the tuning of the properties of those thermosets is usually achieved by the synthesis of functional allylated monomers.[12,16,36–38] In this study, we used trieugenol phosphate, which we previsously reported, with two different bismaleimides in order to synthesize novel Alder-ene thermosets and to evaluate the influence of the bismaleimide structure on the performances and degradation behavior of the obtained materials. In one hand, we used a commercially available aromatic bismaleimide, the N,N'-1,3-phenylene bismaleimide (PhBMI), in order to obtain high T_g material, and on the other hand, we synthesized a new polydimethylsiloxane-containing bismaleimide (SiBMI), resulting in a very low T_g

material. We analyzed the thermo-mechanical properties and studied the degradation of those thermosets.

Materials and methods

1) Materials

Poly(dimethylsiloxane), bis(3-aminopropyl) terminated ($\overline{Mn} = 2{,}500$ g/mol) (PDMS-amine) was purchased from ABCR, *N,N'*-1,3-phenylene bismaleimide (97 %), Zinc dichloride (98 %), Hexamethyldisilazane (>97 %), eugenol (99 %), phosphorus oxychloride (99 %) and triethylamine (99 %) were supplied by Sigma-Aldrich and were used without purification. Deuterated solvent CDCl$_3$ was obtained from Eurisotop for NMR study. Dichloromethane and toluene were purchased from VWR and used as received.

2) Methods

NMR Analyses: Proton and carbon nuclear magnetic resonance (^{1}H and ^{13}C NMR) analyses were performed in deuterated chloroform (CDCl$_3$) using a Bruker Advance 400 MHz NMR spectrometer at a temperature of 25 °C. NMR samples were prepared as follows: 10 mg of product for ^{1}H experiment in around 0.4 mL of CDCl$_3$. The chemical shifts were reported in part per million. Spin multiplicity is shown by s = singlet, d = doublet, t = triplet, m = multiplet.
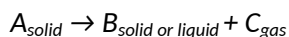
Infrared spectroscopy, for thermoset characterization **:** Attenuated Total Refraction Infrared spectra were recorded on a Nicolet 210 Fourier transform infrared spectroscopy (FTIR) spectrometer with a resolution of 4 cm^{-1}. The characteristic IR absorptions mentioned in the text are reported in cm^{-1}.

Thermogravimetric analyses (TGA), for char determination, were performed using a Netzsch TG 209F1 at a heating rate of 10 °C/min. Approximately 10 mg of monolitic sample was placed in an alumina crucible and heated from room temperature to 900 °C under nitrogen atmosphere (40 mL/min). Nitrogen atomosphere is used in order to reproduce pyrolysis conditions, allowing the formation of char, as described in literature[39].

Thermogravimetric coupled with Fourier-transform infrared (TG-FTIR) analyses, for volatiles characterizations, were performed using a TA Instruments Discovery TGA coupled with Thermo Fischer Nicolet IS10. After a 2 hours isotherm at 40 °C under nitrogen, a heating rate of 10 °C/min was applied until 800 °C. FTIR was performed during the heating ramp, from 4000 to 400 cm^{-1} with a resolution of 4 cm^{-1} (8 scans every 11 s).

Thermogravimetric analyses for degradation kinetics were carried out using a Netzsch TG 209 F1 Libra at five heating rates (1, 2, 5, 10 and 20 °C/min) from 30°C to 800 °C in nitrogen flow (50 mL/min). Samples of exactly 10 mg ($\pm$ 0.3 mg) were put in open alumina pans. Note that according to the good practice of TGA, it can be reasonably assumed at this mass and at those selected heating rates, the

samples can be considered as thermally thin. Typically, two replicates were run for each sample, and the average was reported. Both the onset (5% mass fraction loss) and peak mass loss rate have an uncertainty of 0.9°C (2σ). We corrected for each heating rate the buoyancy force (calibration with empty pan). Kinetic analysis and modeling of the degradation of the samples was made using an advanced thermokinetic software package (Kinetics Neo) developed by Netzsch Company.[40] For kinetic analysis, it is assumed that the material decomposes according to the Equation 1:

$$A_{solid} \rightarrow B_{solid\ or\ liquid} + C_{gas}$$

Equation 1

The rate expression $d\alpha/dt$, where α is the degree of conversion, is assumed to be defined by Equation 2:

$$d\alpha/dt = k(T).f(\alpha)$$

Equation 2

where k is the kinetic constant, $k = A.exp(-E/RT)$ according to the Arrhenius law, A is the frequency factor, E is the activation energy and $f(\alpha)$ is the so-called "reaction model". All reactions are assumed to be irreversible. In the case of decomposition and since the evolved gases were continuously removed by the fluid flow in the TGA chamber, this is a reasonable assumption. It is also assumed that the overall reaction (Equation 1) is the sum of individual reaction steps (formal or true step) with constant activation energy, as generally accepted in chemistry. The model can then include competitive, independent and successive reactions. The equations were solved with multivariate kinetic analysis (determination of the parameter via an hybrid regularized Gauss-Newton method or Marquardt method).

Differential scanning calorimetry (DSC) analyses were carried out using a NETZSCH DSC200F3 calorimeter. Constant calibration was performed using indium, *n*-octadecane and *n*-octane standards. Nitrogen was used as the purge gas. Approximately 10 mg of monolithic sample were placed in pierced aluminum pans and the thermal properties were recorded between -150 °C and 150 °C for the PDMS-amine based material and from 20 °C to 300 °C for the other materials at 20 °C/min to observe the glass transition temperature. The T_g values were measured during the second heating ramp to remove the thermal history of the polymer. All the reported temperatures are averaged values of 3 T_g determinations during the same analysis, with uncertainty presented using one standard deviation (1 σ).

Dynamic Mechanical Analyses (DMA) were carried out on Metravib DMA 25 with Dynatest 6.8 software. Uniaxial stretching of samples was performed while heating at a rate of 3 °C/min from ≈ T_g - 125 °C to T_g 25 °C for SiBMI-based material and from 30 °C to 320 °C for PhBMI-based material, keeping frequency at 1 Hz with a fixed strain of 10^{-5} m. This dynamical strain has been chosen to keep the material on its elastic domain with reversible mechanical stress. All sample were dimensioned according to specification from Metravib, respecting ISO6721.4 standard. PhBMI Thermoset sample was 9 mm×8.34 mm×3.4 mm (height×width×thickness) and SiBMI was 12 mm×4.4 mm×2.1 mm.

Swelling index: Three samples of around 30 mg each were separately put in THF for 24 h. The swelling index (SI) was calculated using the Equation 3 where m_1 is the mass of the material after swelling in THF and m_2 is the initial mass of the material.

$$Equation\ 3 \qquad SI = \frac{m_1 - m_2}{m_2} \times 100$$

Gel content: After SI measurements, the three samples were dried in a ventilated oven at 70 °C for 24 h. The gel content (GC) was calculated using the Equation 4, where m_3 is the mass of the material after the oven and m_2 is the initial mass of the material.

$$Equation\ 4 \qquad GC = \frac{m_3}{m_2} \times 100$$

3) Monomers/Polymers syntheses

   a. Synthesis of monomers

      i. Trieugenylphosphate (TEP) and *N,N'*-1,3-phenylene bismaleimide (PhBMI)

Trieugenylphosphate monomer has been synthesized according to our previsou reported work,[32] and is abbreviated TEP. *N,N'*-1,3-phenylene bismaleimide is commercially available and was used as received, and is abbreviated PhBMI in this article.

      ii. Synthesis of new PDMS-containing bismaleimide (SiBMI)

PDMS-based bismaleimide is a linear maleimide terminated polydimethylsiloxane, abbreviated SiBMI. It was synthesized according to the following procedure, adapted from the literature:[41] Maleic anhydride (4.66 g, 47.5 mmol) was dissolved in 100 mL of dichloromethane (DCM) in a 250 mL round-bottom flask. Then a solution of 20 g (8 mmol) of poly(dimethylsiloxane), bis(3-aminopropyl) terminated ($\overline{Mn} = 2,500$ g/mol) (PDMS-amine) in 40 mL of DCM was added dropwise to the maleic anhydride solution, at ambient temperature, and stirred for 1h. Then, solvent was removed under reduced pressure. The isolated mixture was dissolved in 100 mL of toluene. Then, zinc dichloride (6.5 g, 47.7 mmol) and hexamethyldisilazane (7.6 g, 47.1 mmol) were added to the solution, and heated at

80°C for 5h. The resulting mixture was filtered, and the solvent was removed under reduced pressure to afford the desired product. ^{1}H NMR (CDCl$_3$): δ = 0.10 (m, 237.5 H, CH$_3$Si), 0.50-0.55 (m, 5.4 H, CH$_2$Si), 1.60-1.64 (m, 5.3 H, CH$_2$CH$_2$CH$_2$), 3.52 (t, J = 7.2 Hz, 4.7 H, NCH$_2$), 6.71 (s, 4 H, HC=CH).

b. Polymers synthesis

In order to obtain homogeneous mixtures, monomers have been mixed under vacuum with a Speedmixer DAC 400.2 VAC-P for 5 min at 2500 rpm.

i. Curing of TEP/PhBMI system

A mixture of 2.2 g (4.1 mmol) of TEP and 1.8 g (6.7 mmol) of PhBMI (1 eq of allyl function per eq of maleimide function) has been poured in small PTFE molds. Samples have been cured under vacuum in order to remove air bubbles. A slow curing program with a low temperature ramp (1h at 50 °C, 1h at 80 °C, 1h at 100 °C, 1h at 120 °C, 1h at 150 °C and 180°C overnight) have been chosen instead of a high temperature isotherm curing (200°C) since the latter results in the trapping of air bubbles, which did not happen with the slow program. The resulting cured material appeared as a very hard transparent brown to yellow material.

ii. Curing of TEP/SiBMI system

A mixture of 200 mg (0.37 mmol) of TEP and 2 g (0.75 mmol) of SiBMI (1 eq. of allyl function per eq of maleimide function) was poured into a rectangle silicone mold. The sample has been cured at 180 °C for 24 hours. We obtained a smooth dark brown material.
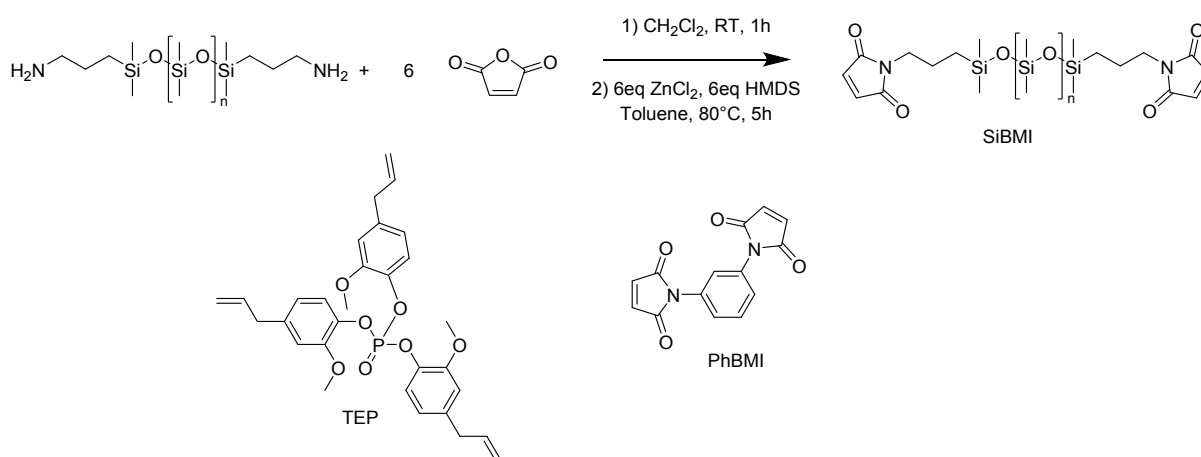

Figure 1 : Pictures of the cured materials.

Results and discussion

1) Description of monomers, synthesis and characterization of the new PDMS-containing bismaleimide

A trifunctional monomer is obtained using a phosphate group, substituted by three eugenol moieties. Thus, the triallyl monomer (trieugenylphosphate) has been synthesized according to our previous work.[32] It shall be noted that this synthesis has also been described using water as the solvent.[42] In addition, another advantage of this phosphorus containing triallyl monomer is that phosphate promotes charring and stabilizes char from oxidation. The commercially available bismaleimide is composed of a six-membered aromatic ring with two maleimide moieties in 1,3 positions. The PDMS containing bismaleimide (SiBMI) has been synthesized by reaction of a commercially available PDMS diamine (with a molar mass of 2,500 g/mol) with maleic anhydride (Scheme 1). In Figure 2 are presented ^{1}H NMR spectra of maleic anhydride, PDMS-diamine and synthesized PDMS bismaleimide. In the ^{1}H NMR spectrum of SiBMI (Figure 2, blue spectrum), the singlet e at 6.71 ppm has been assigned to newly formed maleimide double bond protons, and we can observe that the e" singlet at 7.04 ppm from the maleic anhydride has disappeared in the BMI spectrum. Triplet d at 3.52 ppm is assigned to methylene protons in the alpha position of the amine moiety. The shift of the protons from the amine $d"$ in the red spectrum can be observed, which confirms the addition to the anhydride. Multiplet c around 1.60 ppm is assigned to middle methylene of the aminopropyl residue and 0.55-0.50 ppm multiplet signal b is assigned to the methylene in alpha position of the PDMS chain. The intense signal a at 0.10 ppm is assigned to the methyl protons of the polydimethylsiloxane chain. These attributions confirm that the corresponding maleimide is formed, and that no amine or anhydride is present in the product.

Scheme 1 : Synthesis of SiBMI and chemical structures of TEP and PhBMI.
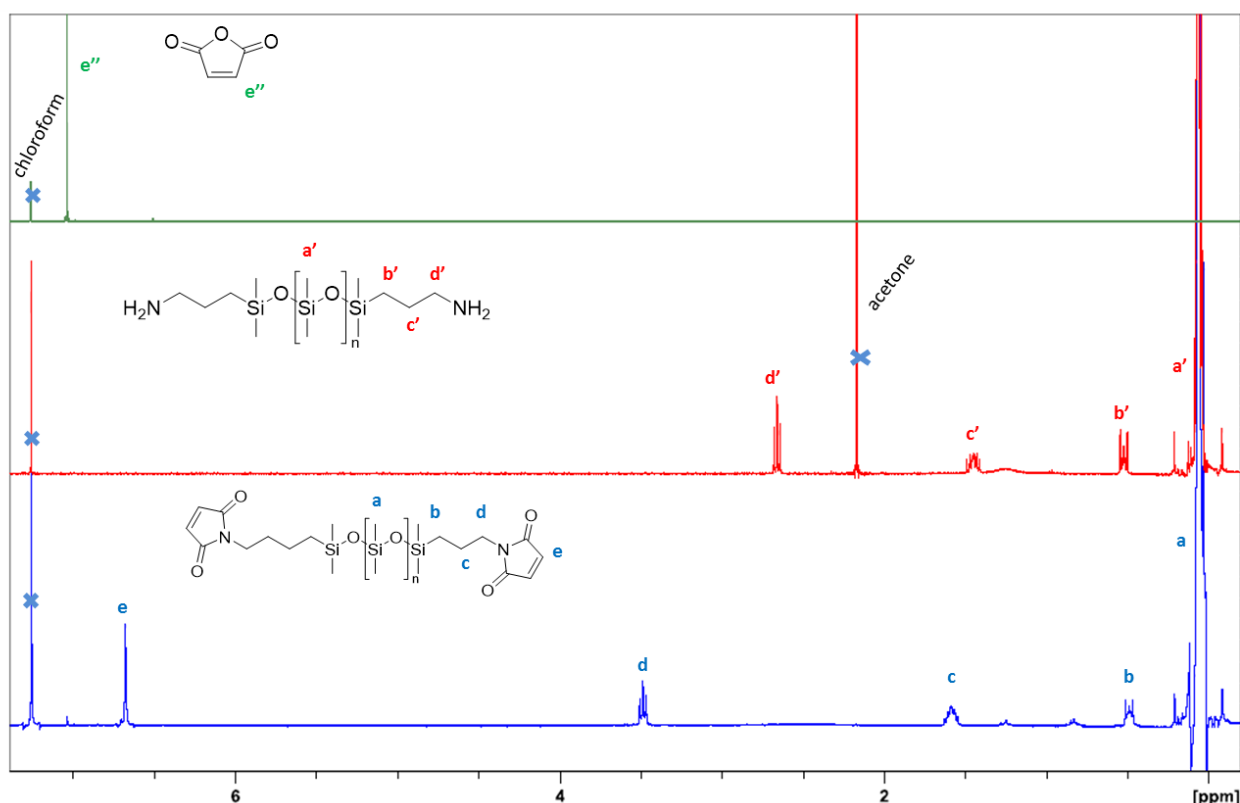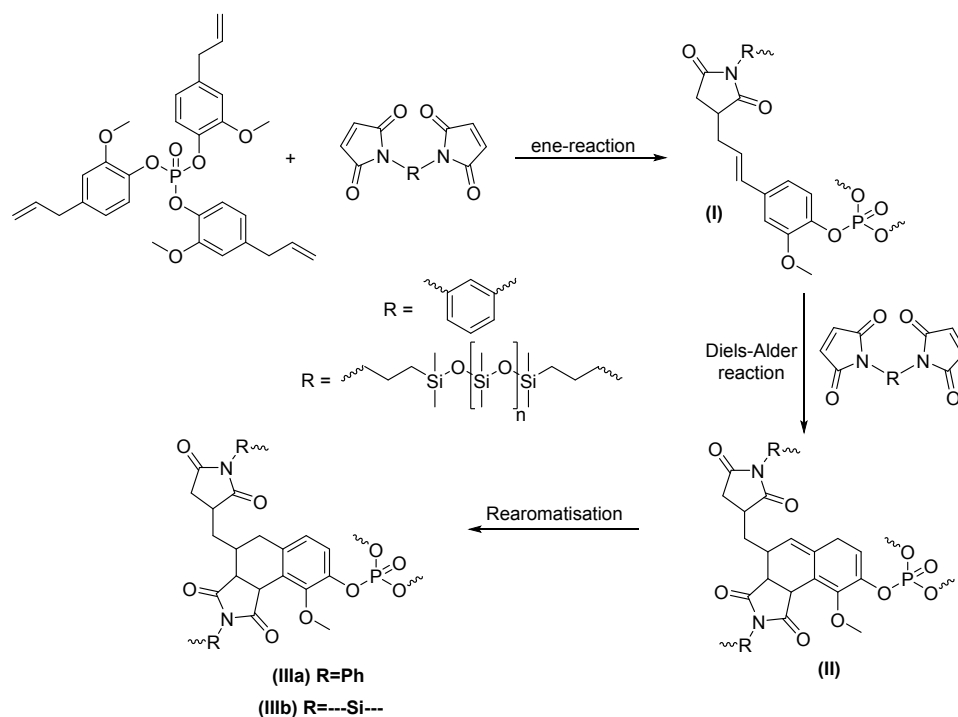
Figure 2: Stacked ¹H NMR spectra of maleic anhydride (top), PDMS-diamine (middle) and PDMS bismaleimide (bottom).

2) Characterization and properties of thermosets

The trifunctional allyl monomer (TEP) has been reacted with both bismaleimides: the aromatic one (PhBMI) and the PMDS-based one (SiBMI) following the synthetic pathway shown in Scheme 2. Firstly, an ene reaction is performed to obtain compound (I) containing intern unsaturation which acts as a diene in a Diels-Alder (DA) reaction. Hence, the maleimide moiety acting as a dienophile in DA reaction, reacts with (I) to form the intermediate (II). Then, a thermal re-aromatization takes place to form the aromatic species (III). These reactions led, if an aromatic bismaleimide is used, to a rigid thermoset (IIIa) due to the presence of many aromatic moieties. On the contrary, the use of a silicon-based bismaleimide led to a flexible material (IIIb) with low glass transition temperature.

Since all these reactions occur during the formation of the thermosets, the curing temperature is crucial. In fact, the homopolymerization takes place at high temperature and consumes the maleimide function.[9] Furthermore, the aromatic bismaleimide is hard to process because it is a solid compound. A slow raise of the temperature up to 200 °C under vaccum was performed to avoid the formation of

bubbles in the thermoset, and it was kept overnight at that temperature and under vacuum. In the case of the use of the PDMS-bismaleimide, which is liquid, these precautions were not necessary and the temperature was only kept constant at 200 °C for 24 hours. Bulk materials have been molded in order to perform thermal and physico-mechanical tests.

Scheme 2 : Synthetic pathway for the formation of thermosets.

An infrared analysis was performed to characterize the thermosets. The spectra were compared to those of TEP monomer and bismaleimide compounds. Figure 3 shows the comparison between the TEP monomer, the PhBMI and the corresponding obtained thermosets (IIIa).

In Figure 3, the absorption bands associated with the unsaturation of allyl function (1444 and 976 cm^{-1}) decreased and the one of the unsaturation of the maleimide (867 cm^{-1}) totally disappeared.[15] In the spectrum IIIa, different characteristic bands appeared. The band at 952 cm^{-1} can be assigned to the stretching vibration of the intermediate trans-olefinic product coming only from the ene-reaction (Scheme 2-(I)).[43] In fact, if the intermediate (II) were isolated, an absorption band between 790 and 840 cm^{-1} should be observed. Thus, this intermediate immediately turns into thermal re-aromatization and is not observed. Many absorption bands, corresponding to the formation of C-C bonds, were observed (1155, 1270 and 1495 cm^{-1}) demonstrating that the Diels-Alder reaction was performed.

The IR spectrum of the PDMS thermoset was not relevant because the high intensity of the bands corresponding to the silicon moiety hides the other signals.
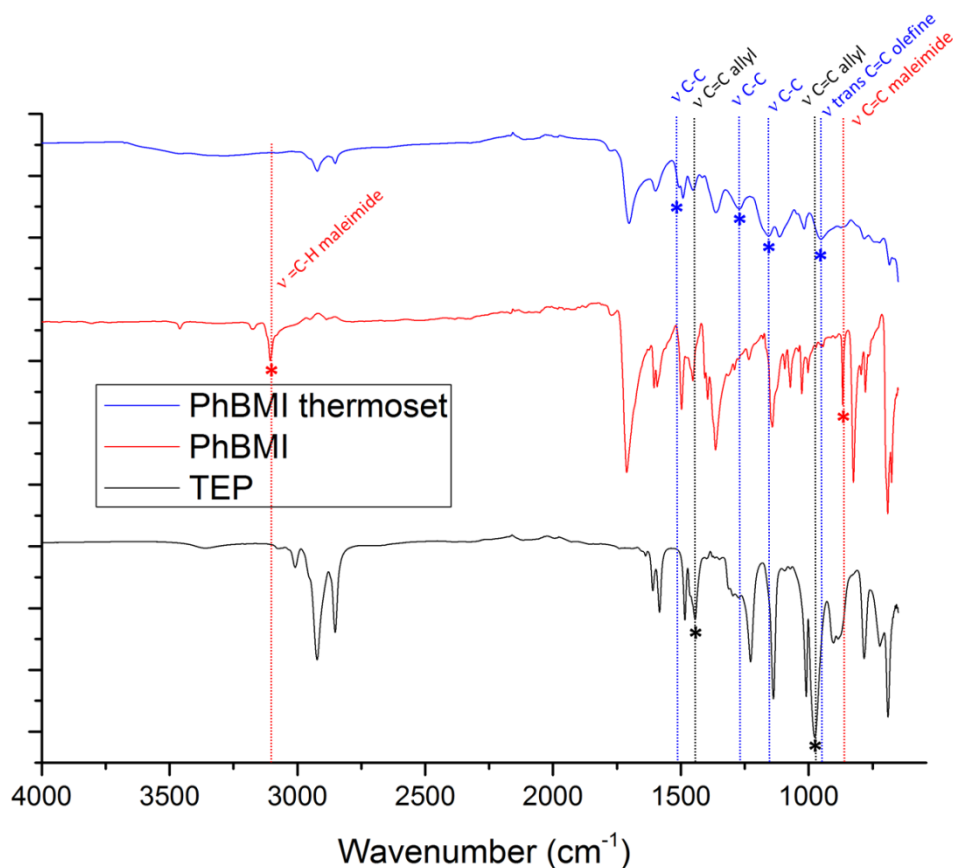
Figure 3 : Stacked infrared spectra of TEP (top), PhBMI (middle) and PhBMI thermoset (bottom).

The cross-linking degree of the network has been characterized with gel content (GC) and swelling index (SI) measurements (Table 1). Gel content corresponds to the residual mass of materials after immersion in THF. With value of 100%, cross-linking is complete for the PhBMI thermoset without any free species trapped in the network. The silicon material presents lower GC values corresponding <mark>to the</mark> presence of non fully reacted PDMS chains. Swelling index is an indication of the cross-linking density and the penetration of the solvent inside the material. The PhBMI thermoset exhibits the lowest swelling index. In fact, the cross-linking density of the SiBMI material is lower than the one of PhBMI thermoset due to high <mark>molar mass</mark> of the PDMS maleimide. Thus, the solvent has easier access into the SiBMI material.

<mark>Thermal measurements have been achieved to examine thermal properties of each material and are summarized in Table 1. TGA measurements were carried out under inert atmosphere to characterize thermal stability of the materials. The 5 %wt degradation occurred over 350 °C in both cases (Table 1). For the silicon thermoset IIIb, it is well-known that the Si-O bond confers a high thermal stability to the</mark>

material thanks to its high bond energy (796 kJ.mol^{-1}).[44] For the PhBMI thermoset IIIa, the high aromaticity content of the material also provides high thermal stability.[45] Furthermore, this high aromaticity entails high char yield (60 %) while a residual mass of 20 % was obtained when the silicon monomer was used. Actually, under an inert atmosphere, depolymerization of the PDMS occurred via the formation of volatile cyclic oligomers during the rupture of the Si-O bond.[46] Furthermore, the rupture of the Si-C bond allows the formation of ceramic silicon-oxycarbide which could lead to some residues. [47] In addition, the presence of phosphate moiety (*i.e* in TEP) in thermosets is well known to enhance char formation in pyrolysis conditions. [48,49]

Table 1 : Thermal and thermo-mechanical properties of materials

	Phosphate content (wt%)	Swelling Index (%)	Gel content (%)	T_g (°C)	$T_{d5\%}$ (°C)	Residual mass (%)	$T\alpha$ (°C)	E'glassy (GPa)	E'rubbery (MPa)
PhBMI thermoset IIIa	10.0	137	100	247 ± 3	359	60	275	1.49 ± 0.01	-
SiBMI thermoset IIIb	1.6	407	91	-113 ± 1	381	20	-114	-	4.4 ± 0.7

Thermo-mechanical properties of the two different materials have been compared by dynamical mechanical analysis (DMA) and the results are outlined in Table 1. The storage modulus (E') and tan δ as function of the temperature for both PhBMI and SiBMI thermosets are shown in Figure 4 and Figure 5 respectively. The alpha-transition temperatures have been measured at the maximum of the tan δ for each material. Tα values followed the same trend as T_g values measured by DSC. Narrow peak of tan δ for SiBMI-based materials shows a good homogeneity of the materials but the tan δ of PhBMI material exhibits a wide peak. This can be explained by the high aromaticity of the PhBMI thermoset which makes the diffusion of the monomers harder than in the SiBMI material. Thus, at room temperature the SiBMI thermoset is in its rubbery domain while the PhBMI material is in its glassy domain. Hence, at room temperature, the PhBMI thermoset is stiff (E'$_{glassy}$ = 1.49 ± 0.01 GPa) while the SiBMI thermoset is more flexible (E'$_{rubbery}$ = 4.4 ± 0.7 MPa).
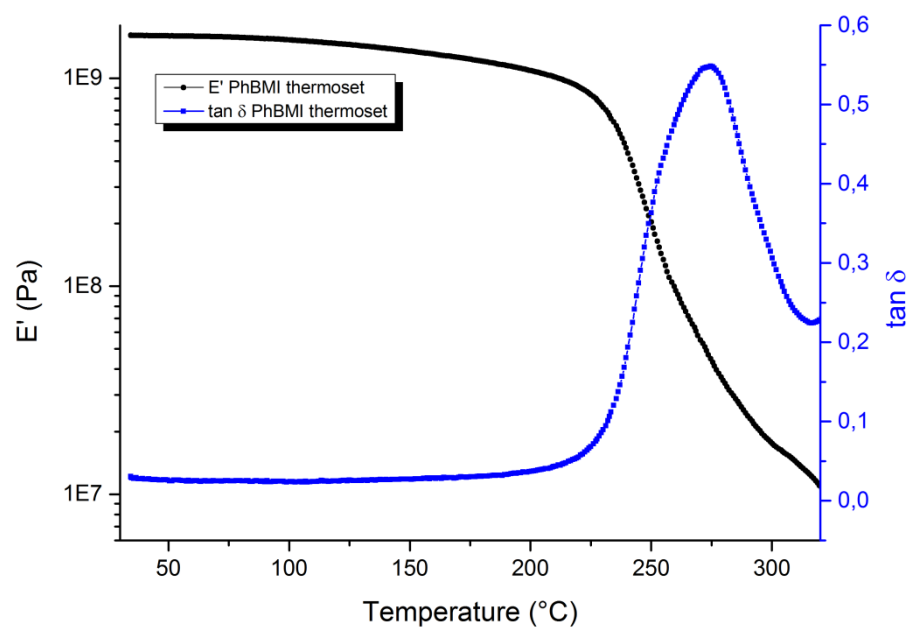
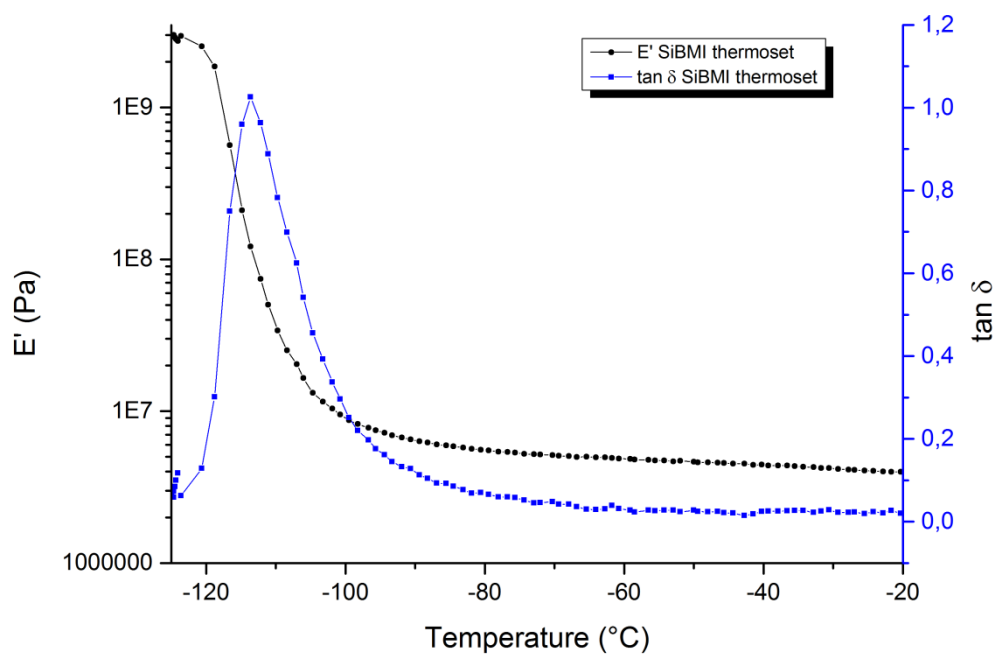*Figure 4: E' (dots) and tan δ (squares) of DMA curves for PhBMI thermoset.*

Figure 5 : E' (dots) and tan δ (squares) of DMA curves for SiBMI thermoset.

Finally, DSC measurements revealed a high glass transition temperature value (247 ± 3 °C) of the PhBMI material because of its high aromaticity content while a very low glass transition temperature (-113 ± 1 °C) was obtained with the SiBMI elastomer due to the presence of flexible segments.

3) Degradation behavior and kinetics analysis

It is known that phosphorus can act as a flame retardant in both gas and condensed phases.[50] TGA-FTIR has been performed in order to characterize the degradation products in pyrolysis conditions to gather data supporting the kinetic analysis discussed hereafter. 3D FTIR plots are presented in Figure 6 for both thermosets. Degradation of SiBMI thermoset shows an apparent single step decomposition occuring between 365 °C and 665 °C. Figure 7 shows the co-added FTIR spectra during this step and only decomposition products of the PDMS chains are detected: the 2969 cm^{-1} band is assigned to C-H bond vibration from the methyl moiety of PDMS, 1265 cm^{-1} band to C-H bond of SiCH$_3$, 1025 cm^{-1} band to Si-O-Si bonds and 815 cm^{-1} band to Si-O-C bonds. We can also observe at 3015 cm^{-1} a weak band corresponding to methane formed by a Si-CH$_3$ homolytic bond scission.[51] Degradation behavior of PhBMI thermoset is more complex, as shown by the TGA thermogram and FTIR analysis of volatiles (Figure 6-(a) and Figure 8). Until 340 °C, no volatiles are detected by FTIR. From 340 to 400 °C, a first significant weight loss is observed on TGA curve and broad bands at 2107 and 2178 cm^{-1} evidence the presence of CO. Hydrocarbons are also present with bands between 2800 and 3000 cm^{-1} and phosphorus-containing volatiles are detected, as shown by presence of bands at 1032 (P-O-C) and 1062 cm^{-1} (P=O) and as previously reported beforehands for bismaleimide-TEP thermoset.[35] Between 430 and 540 °C, CH$_4$ and CO are still observed, and CO$_2$ is detected by bands at 2309 and 2351 cm^{-1} and presence of methane is shown by sharp band at 3015 cm^{-1} in the IR spectrum. Between 730 and 800 °C, CO and CO$_2$ are detected. Water is present at all degradation stages and its signature is very intense starting from 340 °C: it avoids the detection of other degradation products due to the overlapping bands from water. We can conclude that PhBMI thermoset degradation products are mainly simple gases such as water, methane, carbone dioxide and monoxide, which is consistent with the fact that char yield is high. In addition, it is known that depending on the oxidation state of phosphorus in polymer matrix, volatiles observed by TGA-FTIR are different. Phosphates containing phenoxide moieties, such as in TEP, lead to an increased water release compared to phosphorus-containing building blocks without phenoxide. However, no phosphorus-containing compounds are detected when polymer matrix is an epoxy.[49,50] In our case no phosphorus in gas phase was observed in SiBMI thermoset whereas for PhBMI thermoset, some phosphorus species were observed in the early stage

of degradation. It shall be noted that for PhBMI thermoset, phosphate moiety (PO$_4$) represents nearly 10 wt% of the final material, whereas for SiBMI thermoset PO$_4$ represents only 1.6 wt%. Thus, phosphorus may not be detected in the case of SiBMI thermoset because of its very small amount. On the other hand, IR bands of silicon-containing volatiles may superpose to phosphorus-containing ones, in fact the SiBMI owns 77 wt% of silicon unit (Si-O-Me).
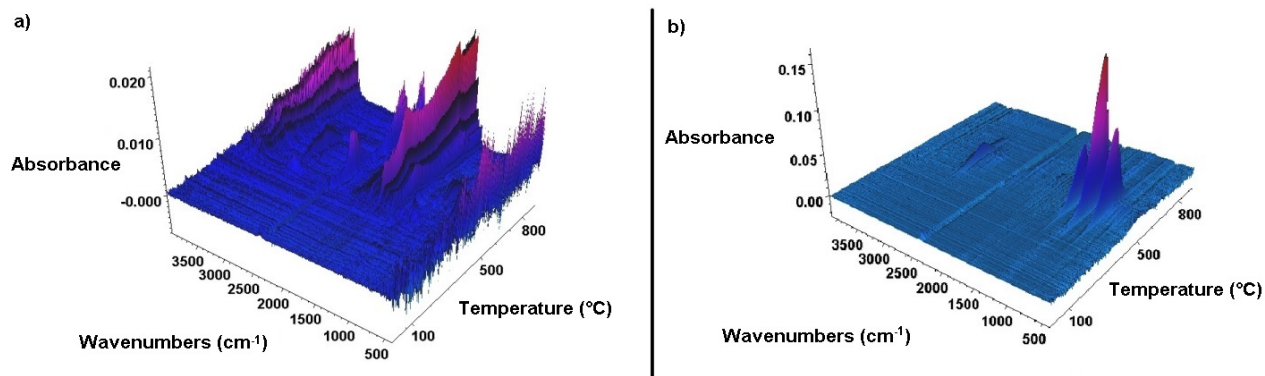

Figure 6 : 3D FTIR spectra of the volatiles products during TG analysis of PhBMI thermoset (a) and SiBMI thermoset (b)
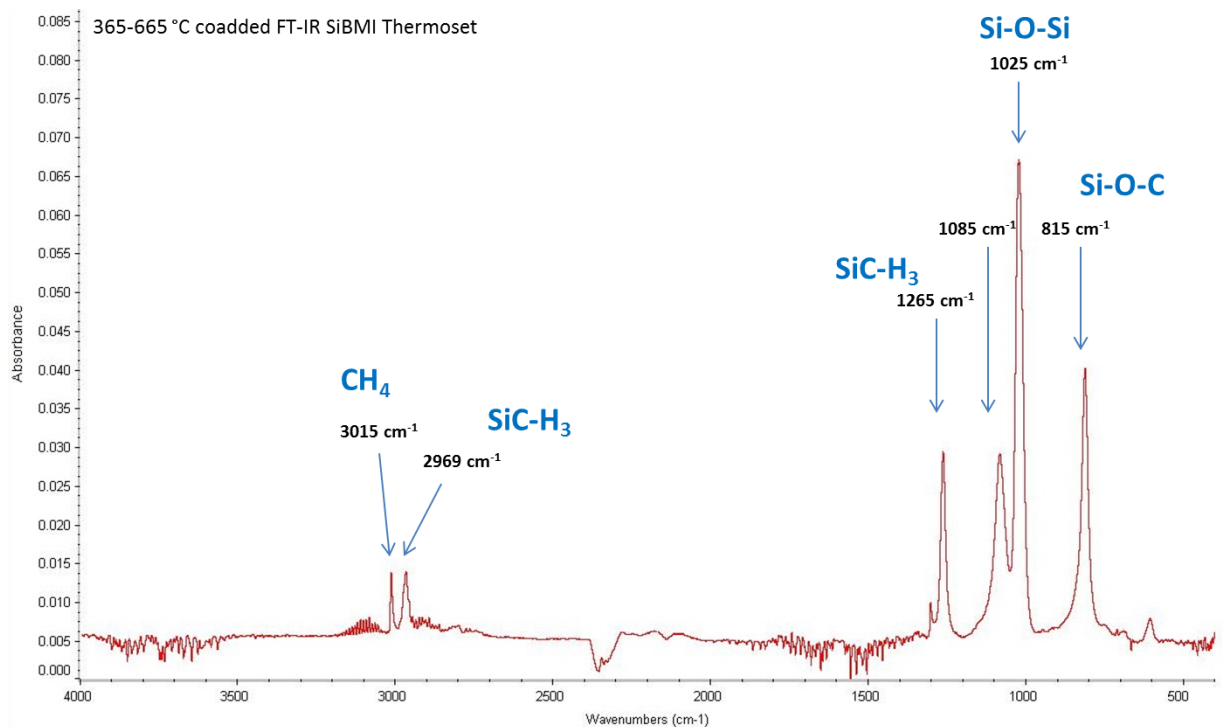
Figure 7 : FTIR spectrum of SiBMI thermoset during TGA between 365 and 665 °C (coadded spectrum)
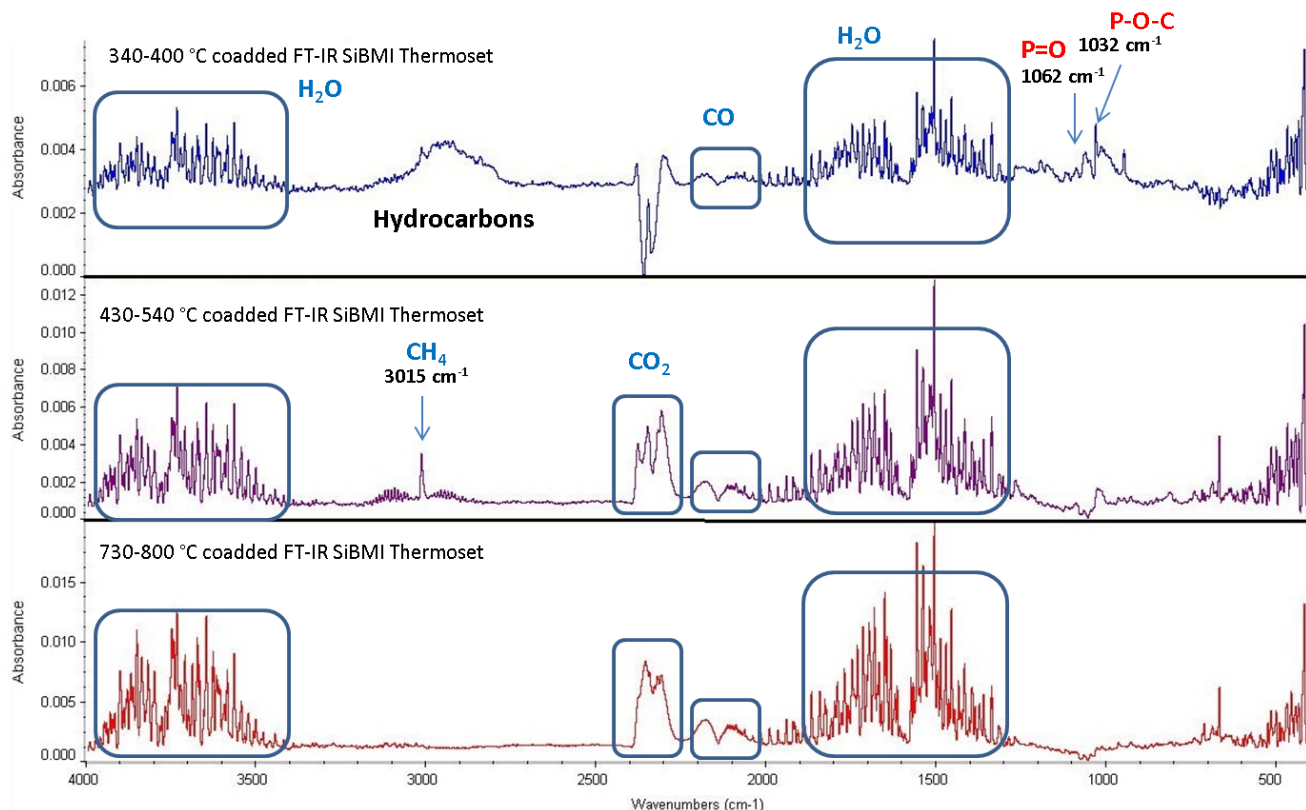
Figure 8 : FTIR spectrum of PhBMI thermoset during TGA at different stages of decomposition (coadded spectrum)

Kinetic analyses were performed on the thermal decomposition of the two thermosets (SiBMI and PhBMI thermosets) to get kinetic parameters, namely the triplet including the frequency factor (A), the activation energy (E) and the reaction order (n). Before starting any fitting procedure, it is necessary to define a model (combination of reactions) and to preset starting values for the kinetic parameters. A convenient approach is to use model-free analysis as a preliminary step of the kinetic analysis such as Friedman analysis.[52] A model-free analysis provides the plot of the activation energy versus the conversion degree. The two materials exhibit different behaviors. For SiBMi thermoset, the activation energy always increases as a function of conversion degree from 100 kJ/mol at low conversion degree to 450 kJ/mol at high conversion degree (Figure 9-(a)). On the other hand, the Friedman plot of PhBMI thermoset shows a plateau of activation energy about 620 kJ/mol up to a conversion degree of 0.8 and instability at higher conversion degree. The causes at the origin of those instabilities (PhBMI and SiBMI) can be multiple such as experimental and calculation system errors, thermal lag, temperature gradient, compensation effect, etc.[53] In the two cases, the Friedman plots indicate that the decomposition does not take place as a one-step reaction but as multi-step reactions.
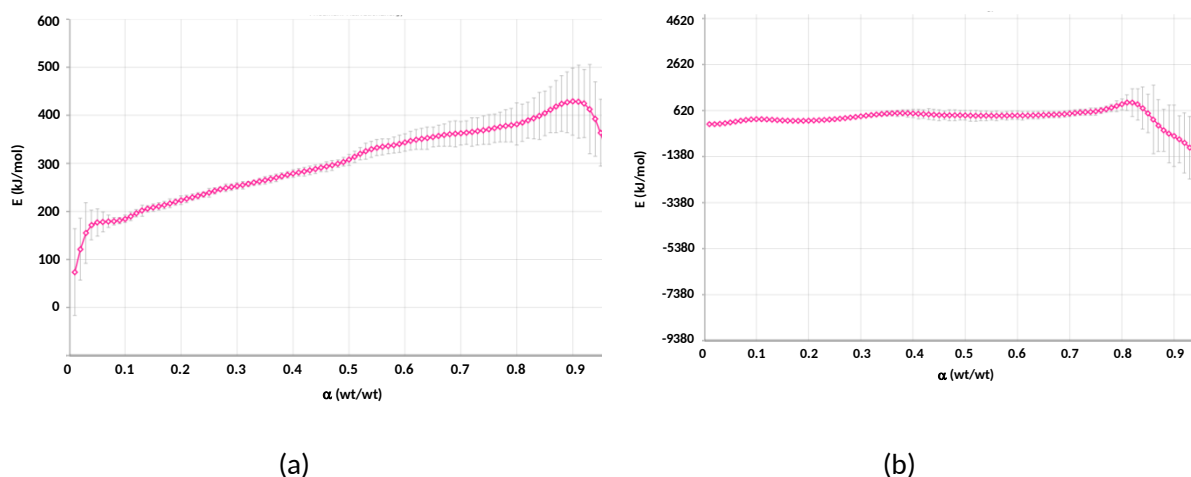
18

Figure 9 - Typical Friedman plots showing activation energies as a function of conversion degrees of (a) SiBMI thermoset and (b) PhBMI thermoset.

TG curve of SiBMI thermoset (Figure 10) shows an apparent single step of decomposition but the Friedman analysis suggested a multi-step decomposition. The simulation of the curves including only one single step does not give satisfactory results (result not shown). The combination of two successive reactions considering Avrami-Erofeev function gives a reasonable fit (Figure 11). The number of steps and the resulting calculated kinetic parameters (Table 2) are consistent with the values of activation energy calculated from the Friedman analysis. According to our modeling, the first step of decomposition contributes for 87 % and is therefore the main step of the decomposition of the SiBMI thermoset. According to TGA-FTIR analysis previously discussed, this step can be assigned to the decomposition of the PDMS chain contained in the thermoset. The calculated activation energy of 275 kJ/mol is consistent with a previous work on the kinetic analysis of the thermal decomposition of polysiloxane.[54] It was also reported that BMI-based thermoset decomposes in several steps with activation energy ranging between 150 and 350 kJ/mol, but no carbonaceous compounds were detected in FTIR.[55,56] The second step contributing at 13 % could be assigned to the species containing the maleimide ring.[57] It is consistent with the activation energy calculated at 400 kJ/mol, even if TGA-FTIR does not evidence this assumption. In SiBMI thermoset, nearly 77 % of the mass originates from the PDMS chains, so it is resonable to assume that some carbon or phosphorus-containing volatiles may not be detected. It has to be noted that this high value is also explained by the presence of phosphorus, due to high degradation bond energy compared to silicon or carbon-containing parts,[58] thus promoting char yield.
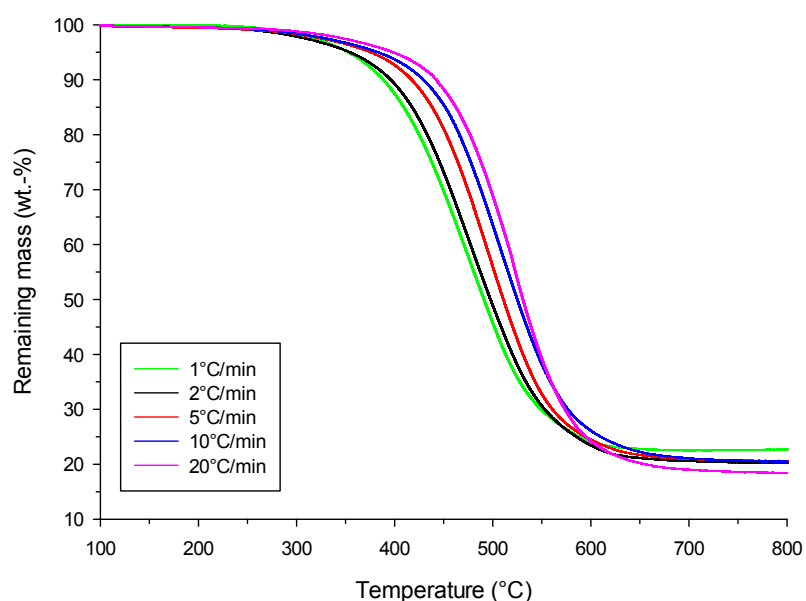
Figure 10 - TG curves of SiBMI thermoset as a function of heating rate (N2 flow)
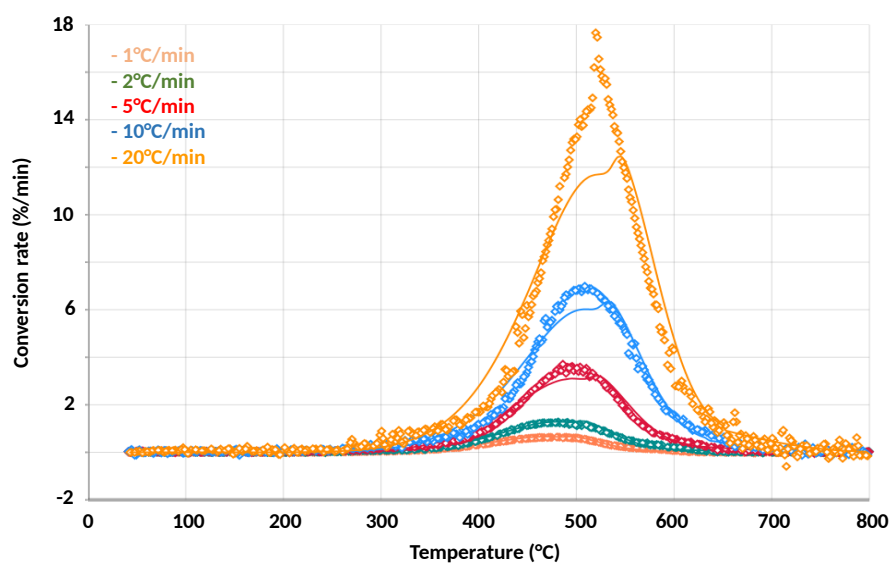

Figure 11 - Experimental and simulated DTG curves of SiBMI thermoset

TG curves of PhBMI thermoset (Figure 12) show a multi-step decomposition which seems more complex than that of SiBMI thermoset. The decomposition was simulated using three successive reactions considering Avrami-Erofeev reaction model (Figure 13). The fit cannot capture all the shape of the curve but it could not be improved using more complex reactional scheme or other reaction models. Table 2 shows the calculated kinetic parameters. The first step (16 %) is assigned to the

degradation of the methylene and allyl group in the structure as reported in literature.[59] It is consistent with TGA-FTIR evidencing the evolution of hydrocarbons and CO. It has to be noted that the activation energy is quite high because of the high number of crosslinks. The second step exhibits a much lower activation energy (128 kJ/mol vs. 281 kJ/mol) than the first step and its contribution is of 43 %. It corresponds to the decomposition of some maleimide part of the material and the volatilization of the remaining decomposed products.[59] Once again, TGA-FTIR supports this assignment showing the evolution of hydrocarbons, CO and CO_2. The third step, which contributes to 41 % of the decomposition, is assigned to the remaining maleimide rings as mentioned in the case of SiBMI thermoset. The activation energy is quite high (381 kJ/mol) and is similar to that of SiBMI thermoset. The reason for this high value is explained by the presence of phosphorus as mentioned above.
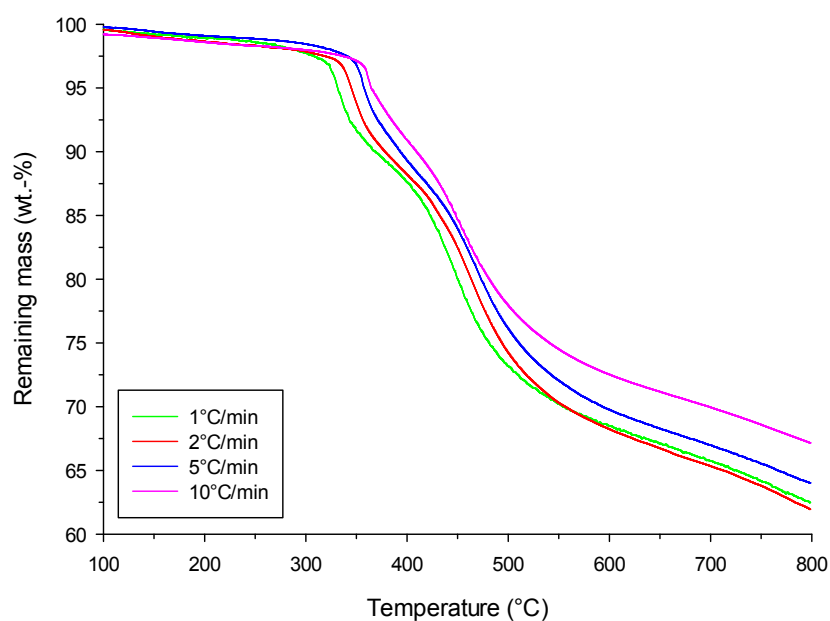

Figure 12 - TG curves of PhBMI thermoset as a function of heating rate (N_2 flow)
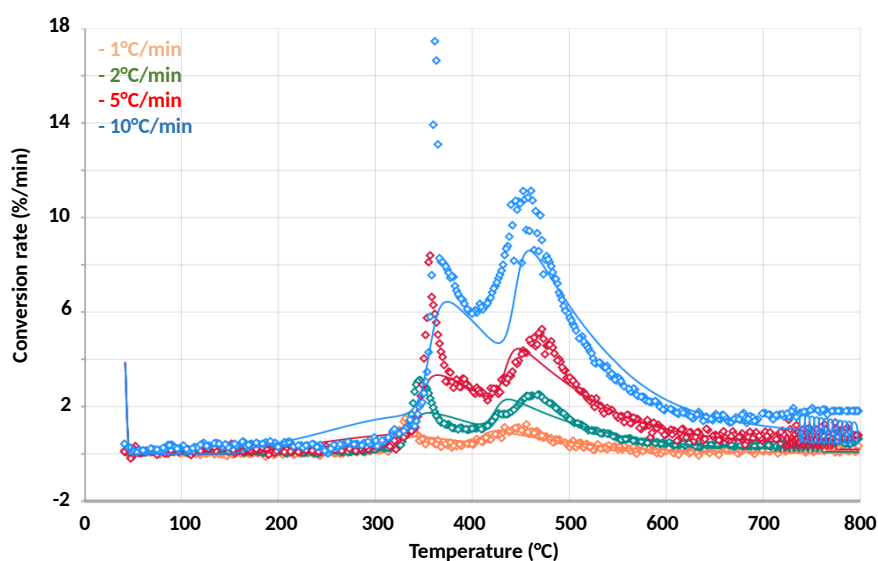
Figure 13 - Experimental and simulated DTG curves of PhBMI thermoset.

Table 2 - Computed kinetic parameters of the decomposition of SiBMI and PhBMI thermosets

Reaction N°	log(A) (A: s^{-1})	E (kJ/mol)	Dimension	Contribution to decomposition
SiBMI thermoset				
1	16 ± 0.9	275 ± 10	0.3 ± 0.1	87%
2	23 ± 1.8	400 ± 18	0.2 ± 0.1	13%
PhBMI thermoset				
1	22 ± 1.9	281 ± 12	0.2 ± 0.1	16%
2	7 ± 0.7	128 ± 8	0.1 ± 0.07	43%
3	25 ± 2.2	381 ± 17	0.1 ± 0.07	41%

Conclusion

Two Alder-ene thermosets were synthetized from renewable clove oil. Phosphate triallyl eugenol monomer was reacted with two types of bismaleimides with different structures: aromatic ring or PDMS oligomer, leading to two different Alder-ene thermosets, PhBMI or SiBMI respectively. Thus, these two bismaleimides lead to different thermally stable thermoset networks with various thermal and mechanical properties. The presence of PDMS chain in SiBMI gives a lower T_g (around -113°C) and an important swelling due to the distance between to cross-linking nodes. In the contrary, aromatic

22

group of PhBMI increased strongly the rigidity of the material. Phosphate function improved the production of char for both Alder-ene thermosets with a char yield ranging from 20 % for SiBMI to more than 60% for PhBMI. Moreover, the degradation behaviors were studied by TGA-FTIR and kinetic analysis were made. The presence of silicon signal in the degradation gases for SiBMI did not make it possible to highlight the role of phosphorus in this material contrary to PhBMI. This latter one underwent multi-step degradation with higher total activation energy mainly due to the presence of phosphate function in the thermoset. The high properties of these new thermosets allowed to consider applications in highly demanding domains such as electronics, building or transport to replace toxic formo-phenolic resins.

References

[1]   X. Xiong, R. Ren, P. Chen, Q. Yu, J. Wang, C. Jia, Preparation and properties of modified bismaleimide resins based on phthalide-containing monomer, J. Appl. Polym. Sci. 130 (2013) 1084–1091. doi:10.1002/app.39269.

[2]   R.J. Iredale, C. Ward, I. Hamerton, Modern advances in bismaleimide resin technology: A 21st century perspective on the chemistry of addition polyimides, Prog. Polym. Sci. 69 (2017) 1–21. doi:10.1016/j.progpolymsci.2016.12.002.

[3]   H.D. Stenzenberger, Addition polyimides, in: High Perform. Polym., Springer-Verlag, Berlin/Heidelberg, n.d.: pp. 165–220. doi:10.1007/BFb0021199.

[4]   Y. Yan, X. Shi, J. Liu, T. Zhao, Y. Yu, Thermosetting resin system based on novolak and bismaleimide for resin-transfer molding, J. Appl. Polym. Sci. 83 (2002) 1651–1657. doi:10.1002/app.10073.

[5]   S. Takeda, H. Kakiuchi, Toughening bismaleimide resins by reactive liquid rubbers, J. Appl. Polym. Sci. 35 (1988) 1351–1366. doi:10.1002/app.1988.070350520.

[6]   A. Chaplin, I. Hamerton, H. Herman, A.K. Mudhar, S.J. Shaw, Studying water uptake effects in resins based on cyanate ester/bismaleimide blends☐, (2000) 12.

[7]   R.J. Iredale, C. Ward, I. Hamerton, Modern advances in bismaleimide resin technology: A 21st century perspective on the chemistry of addition polyimides, Prog. Polym. Sci. 69 (2017) 1–21. doi:10.1016/j.progpolymsci.2016.12.002.

[8]   M. Satheesh Chandran, C.P. Reghunadhan Nair, Maleimide-Based Alder-Enes, in: Handb. Thermoset Plast., Elsevier, 2014: pp. 459–510. doi:10.1016/B978-1-4557-3107-7.00012-9.

[9]   D. Reyx, I. Campistron, C. Caillaud, M. Villatte, A. Cavedon, Thermal reaction between N-phenylmaleimide and 2-allylphenol as a model for the crosslinking reaction in bismaleimide polymerization with diallylbisphenol A, Macromol. Chem. Phys. 196 (1995) 775–785. doi:10.1002/macp.1995.021960308.

[10]   I.D. Cunningham, A. Brownhill, I. Hamerton, B.J. Howlin, The ene reaction between maleimides and allyl-substituted aromatics, Tetrahedron. 53 (1997) 13473–13494. doi:10.1016/S0040-4020(97)00856-9.

[11]   H.D. SterLzenberger, T. GMBH-Verfahrenstechnik, Addition polyimides, (n.d.) 56.

[12]   C. Nair, Advances in addition-cure phenolic resins, Prog. Polym. Sci. 29 (2004) 401–498. doi:10.1016/j.progpolymsci.2004.01.004.

[13]   R.L. Bindu, C.P. Reghunadhan Nair, K.N. Ninan, Addition-cure-type phenolic resin based on alder-ene reaction: Synthesis and laminate composite properties, J. Appl. Polym. Sci. 80 (2001) 737–749. doi:10.1002/1097-4628(20010502)80:5<737::AID-APP1150>3.0.CO;2-V.

[14]   Z. Luo, L. Wei, F. Liu, T. Zhao, The effect of allylation degree on processing properties, thermal cure, and thermal properties of BMAN resins, J. Appl. Polym. Sci. 104 (2007) 2822–2829. doi:10.1002/app.25706.

[15]   J.C. Phelan, C.S.P. Sung, Cure Characterization in Bis(maleimide)/Diallylbisphenol A Resin by Fluorescence, FT-IR, and UV-Reflection Spectroscopy, Macromolecules. 30 (1997) 6845–6851. doi:10.1021/ma961887f.

[16]   A. Tiwari, A.K. Nema, C.K. Das, S.K. Nema, Thermal analysis of polysiloxanes, aromatic polyimide and their blends, Thermochim. Acta. 417 (2004) 133–142. doi:10.1016/j.tca.2003.10.003.

[17]   R.J. Morgan, E. Eugene Shin, B. Rosenberg, A. Jurek, Characterization of the cure reactions of bismaleimide composite matrices, Polymer (Guildf). 38 (1997) 639–646. doi:10.1016/S0032-3861(96)00542-3.

[18]   J.-M. Raquez, M. Deléglise, M.-F. Lacrampe, P. Krawczak, Thermosetting (bio)materials derived from renewable resources: A critical review, Prog. Polym. Sci. 35 (2010) 487–509. doi:10.1016/j.progpolymsci.2010.01.001.

[19]   M. Fache, B. Boutevin, S. Caillol, Vanillin, a key-intermediate of biobased polymers, Eur. Polym. J. 68 (2015) 488–502. doi:10.1016/j.eurpolymj.2015.03.050.

[20]   E.D. Hernandez, A.W. Bassett, J.M. Sadler, J.J. La Scala, J.F. Stanzione, Synthesis and Characterization of Bio-based Epoxy Resins Derived from Vanillyl Alcohol, ACS Sustain. Chem. Eng. 4 (2016) 4328–4339. doi:10.1021/acssuschemeng.6b00835.

[21]   E. Feghali, K.M. Torr, D.J. van de Pas, P. Ortiz, K. Vanbroekhoven, W. Eevers, R. Vendamme, Thermosetting Polymers from Lignin Model Compounds and Depolymerized Lignins, Top. Curr. Chem. 376 (2018). doi:10.1007/s41061-018-0211-6.

[22]   A. Llevot, E. Grau, S. Carlotti, S. Grelier, H. Cramail, From Lignin-derived Aromatic Compounds to Novel Biobased Polymers, Macromol. Rapid Commun. 37 (2016) 9–28. doi:10.1002/marc.201500474.

[23]   S. Zhao, M.M. Abu-Omar, Synthesis of Renewable Thermoset Polymers through Successive Lignin Modification Using Lignin-Derived Phenols, ACS Sustain. Chem. Eng. 5 (2017) 5059–5066. doi:10.1021/acssuschemeng.7b00440.

[24]   L. Yue, F. Liu, S. Mekala, A. Patel, R.A. Gross, I. Manas-Zloczower, High Performance Biobased Epoxy Nanocomposite Reinforced with a Bacterial Cellulose Nanofiber Network, ACS Sustain. Chem. Eng. 7 (2019) 5986–5992. doi:10.1021/acssuschemeng.8b06073.

[25]   S. Caillol, Cardanol: A promising building block for biobased polymers and additives, Curr. Opin.

Green Sustain. Chem. 14 (2018) 26–32. doi:10.1016/j.cogsc.2018.05.002.

[26] X. Pan, D.C. Webster, New Biobased High Functionality Polyols and Their Use in Polyurethane Coatings, ChemSusChem. 5 (2012) 419–429. doi:10.1002/cssc.201100415.

[27] F. Hu, J.J. La Scala, J.M. Sadler, G.R. Palmese, Synthesis and Characterization of Thermosetting Furan-Based Epoxy Systems, Macromolecules. 47 (2014) 3332–3342. doi:10.1021/ma500687t.

[28] A. Arbenz, L. Avérous, Chemical modification of tannins to elaborate aromatic biobased macromolecular architectures, Green Chem. 17 (2015) 2626–2646. doi:10.1039/c5gc00282f.

[29] D.G. Vassão, L.B. Davin, N.G. Lewis, Metabolic Engineering of Plant Allyl/Propenyl Phenol and Lignin Pathways: Future Potential for Biofuels/Bioenergy, Polymer Intermediates, and Specialty Chemicals?, in: Adv. Plant Biochem. Mol. Biol., 2008: pp. 385–428. doi:10.1016/S1755-0408(07)01013-2.

[30] M. Shibata, N. Teramoto, T. Shimasaki, M. Ogihara, High-performance bio-based bismaleimide resins using succinic acid and eugenol, Polym. J. 43 (2011) 916–922. doi:10.1038/pj.2011.87.

[31] M. Neda, K. Okinaga, M. Shibata, High-performance bio-based thermosetting resins based on bismaleimide and allyl-etherified eugenol derivatives, Mater. Chem. Phys. 148 (2014) 319–327. doi:10.1016/j.matchemphys.2014.07.050.

[32] I. Faye, M. Decostanzi, Y. Ecochard, S. Caillol, Eugenol bio-based epoxy thermosets: from cloves to applied materials, Green Chem. 19 (2017) 5236–5242. doi:10.1039/C7GC02322G.

[33] J.-T. Miao, L. Yuan, Q. Guan, G. Liang, A. Gu, Biobased epoxy resin derived from eugenol with excellent integrated performance and high renewable carbon content: Biobased epoxy resin derived from eugenol, Polym. Int. 67 (2018) 1194–1202. doi:10.1002/pi.5621.

[34] S. Li, H. Yan, S. Feng, S. Niu, Synthesis and characterization of a phosphorus-containing flame retardant with double bonds and its application in bismaleimide resins, RSC Adv. 5 (2015) 101480–101486. doi:10.1039/C5RA15946F.

[35] J.-T. Miao, L. Yuan, G. Liang, A. Gu, Biobased bismaleimide resins with high renewable carbon content, heat resistance and flame retardancy via a multi-functional phosphate from clove oil, Mater. Chem. Front. 3 (2019) 78–85. doi:10.1039/C8QM00443A.

[36] X. Zhang, R. Akram, S. Zhang, H. Ma, Z. Wu, D. Wu, Hexa(eugenol)cyclotriphosphazene modified bismaleimide resins with unique thermal stability and flame retardancy, React. Funct. Polym. 113 (2017) 77–84. doi:10.1016/j.reactfunctpolym.2017.02.010.

[37] A. Gu, Novel high performance RTM bismaleimide resin with low cure temperature for advanced composites, Polym. Adv. Technol. 16 (2005) 563–566. doi:10.1002/pat.615.

[38] G. Liang, J. Fan, Novel modified bismaleimide resins with improved ablativity, J. Appl. Polym. Sci. 73 (1999) 1623–1631. doi:10.1002/(SICI)1097-4628(19990829)73:9<1623::AID-APP3>3.0.CO;2-Z.

[39] L. Torre, J.M.M. Kenny, A.M. Maffezzoli, Degradation behaviour of a composite material for thermal protection systems Part I–Experimental characterization, J. Mater. Sci. 33 (1998) 3137–3143. doi:10.1023/A:1004399923891.

[40] J. Opfermann, Kinetic analysis using multivariate non-linear regression. I. Basic concepts, J. Therm. Anal. Calorim. 60 (2000) 641–658. doi:10.1023/A:1010167626551.

[41] T. Engel, G. Kickelbick, Furan-Modified Spherosilicates as Building Blocks for Self-Healing Materials: Furan-Modified Spherosilicates for Self-Healing Materials, Eur. J. Inorg. Chem. 2015 (2015) 1226–1232. doi:10.1002/ejic.201402551.

[42] J.-T. Miao, L. Yuan, Q. Guan, G. Liang, A. Gu, Water-Phase Synthesis of a Biobased Allyl Compound for Building UV-Curable Flexible Thiol–Ene Polymer Networks with High Mechanical Strength and Transparency, ACS Sustain. Chem. Eng. 6 (2018) 7902–7909. doi:10.1021/acssuschemeng.8b01128.

[43] G. Socrates, Infrared and Raman characteristic group frequencies: tables and charts, 3. ed, Wiley, Chichester, 2001.

[44] S. Hamdani, C. Longuet, D. Perrin, J.-M. Lopez-cuesta, F. Ganachaud, Flame retardancy of silicone-based materials, Polym. Degrad. Stab. 94 (2009) 465–495. doi:10.1016/j.polymdegradstab.2008.11.019.

[45] V.V. Korshak, V.A. Khomutov, Y.Y. Doroshenko, A study of thermal stability in a number of aromatic and nitrogen containing polycyclic compounds, Polym. Sci. U.S.S.R. 18 (1976) 597–603. doi:10.1016/0032-3950(76)90253-7.

[46] T.H. Thomas, T.C. Kendrick, Thermal analysis of polydimethylsiloxanes. I. Thermal degradation in controlled atmospheres, J. Polym. Sci. Part A-2 Polym. Phys. 7 (1969) 537–549. doi:10.1002/pol.1969.160070308.

[47] G. Camino, S.. Lomakin, M. Lageard, Thermal polydimethylsiloxane degradation. Part 2. The degradation mechanisms, Polymer (Guildf). 43 (2002) 2011–2015. doi:10.1016/S0032-3861(01)00785-6.

[48] S. Bourbigot, S. Duquesne, Fire retardant polymers: recent developments and opportunities, J. Mater. Chem. 17 (2007) 2283. doi:10.1039/b702511d.

[49] U. Braun, A.I. Balabanovich, B. Schartel, U. Knoll, J. Artner, M. Ciesielski, M. Döring, R. Perez, J.K.W. Sandler, V. Altstädt, T. Hoffmann, D. Pospiech, Influence of the oxidation state of phosphorus on the decomposition and fire behaviour of flame-retarded epoxy resin composites, Polymer (Guildf). 47 (2006) 8495–8508. doi:10.1016/j.polymer.2006.10.022.

[50] B. Schartel, Phosphorus-based Flame Retardancy Mechanisms—Old Hat or a Starting Point for Future Development?, Materials (Basel). 3 (2010) 4710–4745. doi:10.3390/ma3104710.

[51] G. Camino, S.. Lomakin, M. Lageard, Thermal polydimethylsiloxane degradation. Part 2. The degradation mechanisms, Polymer (Guildf). 43 (2002) 2011–2015. doi:10.1016/S0032-3861(01)00785-6.

[52] H.L. Friedman, Kinetics of thermal degradation of char-forming plastics from thermogravimetry. Application to a phenolic plastic, J. Polym. Sci. Part C Polym. Symp. 6 (2007) 183–195. doi:10.1002/polc.5070060121.

[53] M. Carrier, L. Auret, A. Bridgwater, J.H. Knoetze, Using Apparent Activation Energy as a Reactivity Criterion for Biomass Pyrolysis, Energy & Fuels. 30 (2016) 7834–7841. doi:10.1021/acs.energyfuels.6b00794.

[54] G. Caminoa, S.M. Lomakin, M. Lazzari, Polydimethylsiloxane thermal degradation. Part 1. Kinetic aspects., Polymer (Guildf). 42 (2001) 2395–2402. doi:10.1016/0038-1101(90)90239-B.

[55] C. Gouri, C.. Reghunadhan Nair, R. Ramaswamy, K.. Ninan, Thermal decomposition characteristics of Alder-ene adduct of diallyl bisphenol A novolac with bismaleimide: effect of stoichiometry, novolac molar mass and bismaleimide structure, Eur. Polym. J. 38 (2002) 503–510. doi:10.1016/S0014-3057(01)00197-5.

[56] Q.-T. Pham, J.-M. Hsu, J.-P. Pan, T.-H. Wang, C.-S. Chern, Non-isothermal degradation kinetics of N , N ′-bismaleimide-4,4′-diphenylmethane/barbituric acid based polymers in the presence of hydroquinone, J. Appl. Polym. Sci. 130 (2013) 1923–1930. doi:10.1002/app.39360.

[57] Q.-T. Pham, J.-M. Hsu, J.-P. Pan, T.-H. Wang, C.-S. Chern, Synthesis and characterization of phenylsiloxane-modified bismaleimide/barbituric acid-based polymers with 3-aminopropyltriethoxysilane as the coupling agent, Polym. Int. 62 (2012) n/a–n/a. doi:10.1002/pi.4390.

[58] T. Ho, T. Leu, Y. Sun, J. Shieh, Thermal degradation kinetics and flame retardancy of phosphorus-containing dicyclopentadiene epoxy resins, Polym. Degrad. Stab. 91 (2006) 2347–2356. doi:10.1016/j.polymdegradstab.2006.04.002.

[59]   C. Gouri, C.. Reghunadhan Nair, R. Ramaswamy, K.. Ninan, Thermal decomposition characteristics of Alder-ene adduct of diallyl bisphenol A novolac with bismaleimide: effect of stoichiometry, novolac molar mass and bismaleimide structure, Eur. Polym. J. 38 (2002) 503–510. doi:10.1016/S0014-3057(01)00197-5.